Graduate School ETD Form 9
(Revised 12/07)

PURDUE UNIVERSITY
GRADUATE SCHOOL
Thesis/Dissertation Acceptance

This is to certify that the thesis/dissertation prepared

By Umut Tugsal

Entitled FAULT DIAGNOSIS OF ELECTRONIC FUEL CONTROL (EFC) VALVES VIA DYNAMIC PERFORMANCE TEST METHOD

For the degree of Master of Science in Electrical and Computer Engineering

Is approved by the final examining committee:

Yaobin Chen (Co-Chair)
Chair

Sohel Anwar (Co-Chair)

Lingxi Li

To the best of my knowledge and as understood by the student in the *Research Integrity and Copyright Disclaimer (Graduate School Form 20)*, this thesis/dissertation adheres to the provisions of Purdue University's "Policy on Integrity in Research" and the use of copyrighted material.

Approved by Major Professor(s): Yaobin Chen

Sohel Anwar

Approved by: Yaobin Chen 12/02/2009
Head of the Graduate Program Date

Graduate School Form 20
(Revised 6/09)

PURDUE UNIVERSITY
GRADUATE SCHOOL

Research Integrity and Copyright Disclaimer

Title of Thesis/Dissertation:

FAULT DIAGNOSIS OF ELECTRONIC FUEL CONTROL (EFC) VALVES VIA DYNAMIC PERFORMANCE TEST METHOD

For the degree of Master of Science in Electrical and Computer Engineering

I certify that in the preparation of this thesis, I have observed the provisions of *Purdue University Executive Memorandum No. C-22,* September 6, 1991, *Policy on Integrity in Research.**

Further, I certify that this work is free of plagiarism and all materials appearing in this thesis/dissertation have been properly quoted and attributed.

I certify that all copyrighted material incorporated into this thesis/dissertation is in compliance with the United States' copyright law and that I have received written permission from the copyright owners for my use of their work, which is beyond the scope of the law. I agree to indemnify and save harmless Purdue University from any and all claims that may be asserted or that may arise from any copyright violation.

Umut Tugsal

Printed Name and Signature of Candidate

11/24/2009

Date (month/day/year)

*Located at http://www.purdue.edu/policies/pages/teach_res_outreach/c_22.html

FAULT DIAGNOSIS OF ELECTRONIC FUEL CONTROL (EFC) VALVES VIA DYNAMIC PERFORMANCE TEST METHOD

A Thesis
Submitted to the Faculty
of
Purdue University
by
Umut Tugsal

In Partial Fulfillment of the
Requirements for the Degree
of
Master of Science in Electrical and Computer Engineering

December 2009
Purdue University
Indianapolis, Indiana

To my family

ACKNOWLEDGMENTS

I would like to gratefully acknowledge my thesis advisor, Dr. Sohel Anwar, for his assistance, guidance, and supervision during the entire course of this research and thesis work. Dr. Anwar generously shared with me his research experience and directed me towards perfection in every detail, for which I am always thankful.

I would like to thank my co-advisor Dr. Yaobin Chen, and my advisory committee member Dr. Lingxi Li for their time and insight during the completion of this thesis.

I would also like to thank my fellow students at the Mechatronics Laboratory; Mr. Harpreetsingh Banvait, and Mr. Tolga Yildiz for their help and support during this phase of my life. I thank Mrs. Valerie Lim Diemer and Mrs. Sherrie Tucker for assisting me in formatting this thesis.

TABLE OF CONTENTS

Page

Page

LIST OF TABLES

LIST OF FIGURES

Figure Page

Figure Page

ABSTRACT

Tugsal, Umut. M.S.E.C.E., Purdue University, December 2009. Fault Diagnosis of Electronic Fuel Control (EFC) Valves via Dynamic Performance Test Method. Major Professors: Sohel Anwar and Yaobin Chen.

Electronic Fuel Control (EFC) valve regulates fuel flow to the injector fuel supply line in the Cummins Pressure Time (PT) fuel system. The EFC system controls the fuel flow by means of a variable orifice that is electrically actuated. The supplier of the EFC valves inspects all parts before they are sent out. Their inspection test results provide a characteristic curve which shows the relationship between pressure and current provided to the EFC valve. This curve documents the steady state characteristics of the valve but does not adequately capture its dynamic response. A dynamic test procedure is developed in order to evaluate the performance of the EFC valves. The test itself helps to understand the effects that proposed design changes will have on the stability of the overall engine system. A by product of this test is the ability to evaluate returned EFC valves that have experienced stability issues. The test determines whether an EFC valve is faulted or not before it goes out to prime time use. The characteristics of a good valve and bad valve can be observed after the dynamic test.

In this thesis, a mathematical model has been combined with experimental research to investigate and understand the behavior of the characteristics of different types of EFC valves. The model takes into account the dynamics of the electrical and mechanical portions of the EFC valves. System Identification has been addressed to determine the transfer functions of the different types of EFC valves that were

experimented. Methods have been used both in frequency domain as well as time domain. Also, based on the characteristic patterns exhibited by the EFC valves, fuzzy logic has been implemented for the use of pattern classification.

1 INTRODUCTION

1.1 Problem Statement

Cummins, Inc. designs and manufactures a class of Electronic Fuel Control (EFC) [1] rotary electrically actuated valve that is used in Cummins diesel engines. The EFC valve is a rotary electrically actuated proportional valve which regulates fuel flow (rail pressure) to the injector fuel supply line in the Cummins Pressure Time (PT) fuel system. The EFC system controls the fuel flow by providing a variable orifice. The size of the orifice is proportional to the duty cycle (pulse width modulated signal) of supplied voltage. Cummins utilizes normally open and normally closed EFC valves.

The current supplier of the EFC valve inspects all parts 100% before they are shipped to Cummins. Their inspection test results provide a characteristics curve which shows the relationship between rail pressure and current provided to the EFC valve. This curve documents the steady state characteristics of the valve but does not adequately capture its dynamic response.

PT Fuel Systems utilizing the EFC valve actuators are used in a wide variety of engine configurations, primarily for the Stationary Power Plants (Generator Set) and military applications. Since the fuel system uses an older technology, it is often difficult to obtain “on engine” testing to validate design changes to the EFC system or to confirm product quality issues reported by the customers.

A dynamic test procedure must be developed to evaluate the performance of the EFC valves. This test should help understand the effects that the proposed design changes will have on the stability of the overall engine system, without resorting to on – engine

testing. This test should also provide a mechanism to evaluate EFC valves that have been returned from the customer engines and are experiencing stability issues.

1.2 Previous Work

Mechanical systems are often nonlinear with nonlinear components and nonlinear connections. The occurrence of any mechanical damage frequently causes changes in the nonlinear characteristics of mechanical systems, in the end causing the system to become somewhat less stable. As a result, methods which characterize the nonlinear behavior of mechanical systems are well suited to detect such damages and stability issues. The methodologies of time domain and frequency domain have been extensively used to determine the changes in the nonlinear behavior of a mechanical system to identify damages and stability issues. To be more precise, the two aforementioned methodologies help with System Identification.

1.2.1 Frequency Domain

Frequency Domain Methodology (FDM) has been proposed as a technique for factor screening [2] and for gradient estimation [3]. The method uses the Fourier transform of the output process. The identification focuses on estimating the coefficients of the model. The method is tested on a known structure and an unknown structure. The procedure successfully fits the coefficients, including obtaining the correct signs.

A major advantage of FDM is its ability to give information in a region of the parameter space. The idea of the FDM is to oscillate the design factors during runs, rather than holding them fixed as conventional simulation runs do.

This approach has a number of issues. There are design issues for FDM; first and foremost, the choice of the appropriate region of the parameter space. Next, the driving

frequencies for the experimental factors, and finally the appropriate method for estimating the frequency content of the output.

Another method developed out of necessity was the Frequency Domain System Identification with Missing Data [4]. This method was presented as a solution to the problem of missing data in the input signals and the output signals because of temporary sensor failures or data transmission errors.

The main advantages of this method are that it requires no parametric model for the input signal, it is valid for any model structure, and it can be applied to discrete time as well as continuous time models. Basically, the idea is to treat the missing data from the input signals and the output signals as unknown parameters in the identification problem.

This method uses a nonlinear least – squares algorithm to generate consistent estimations of the plant model parameters in the case that the noise model is known. The main issue for this method is the large number of parameters if a lot of data are missing.

An alternative approach is the black–box modeling [5]. Using this method, a frequency dependent equivalent component is identified from measured or calculated frequency responses at its terminals.

These processes enable the approximation of a frequency dependent matrix H(s) with rational functions for the purpose of obtaining a realization in the form of matrices A, B, C, and D as used in state space equations. Vector Fitting approach leads to a realization in the form of a sum of partial fractions with a residue matrix for each pole.

Vector Fitting is a powerful method used for system identification in the frequency domain. It is robust, and available in the public domain, therefore has been used in diverse applications.

The main issue with this method is the fact that it must consider a mathematical problem to identify a terminal model of a linear system based on a given set of frequency domain responses represented by the matrix H(s). If there is an instance when a matrix inversion yields a nonlinear result, then alternative methods must be considered, such as Newton's Nonlinear Least – Squares (NLLS) method, at which point, the method loses its robustness.

1.2.2 Time Domain

For the identification of nonlinear dynamic systems, it is important to guarantee the accuracy, robustness, and computational stability of the identification method. These criteria become more significant with the inclusion of noise in the system. This is why linear and nonlinear filters are used to attenuate noise in order to implement feedback.

Mapping based identification concept [6] is used for the identification of nonlinear systems in the time domain. In principal, realizable filters are used in order to recover the variables that are used to identify the unknown parameters that are needed for the formulation of the identification problem. Basically, nonlinear error mappings are implemented to identify a nonlinear system. This method is computationally stable and accurate, while the parameter convergence is guaranteed. This method is completely automated, computationally stable, robust, and efficient.

Another powerful method is the Recursive Least Squares (RLS) Estimation method. The purpose of this identification method is to identify the model parameters using a given set of data. This is an online activity performed every time a new data point becomes available. The RLS estimation [7, 8, 9] method is the most popular technique to accomplish this.

1.3 Objectives

The objectives of this research project are to extend the earlier works of Gustavsson et al. [7, 8, 9] and explore the works of Pintelon & Schoukens [4] on system identification and model characterization to develop a characteristic model of the EFC actuator, fuel pump, and engine system. This research must also be conducted in the manner to determine the overall dynamic performance requirements for the EFC actuator, fuel pump, and engine system then propose these requirements of the EFC dynamic performance evaluation (in time domain, frequency domain, or both). After the requirements have been determined and met, we develop a test methodology for testing EFC valves using equipment currently available at Cummins Fuel System laboratories; and perform the preliminary testing of the EFC valves based on the aforementioned test methodology for validation purposes as well as data acquisition. From the acquired data, a preliminary analysis must be conducted in order to observe any patterns, signatures, or irregularities should they exist.

The nature of the EFC valve could prove useful for the implementation of fuzzy logic methodology in the area of pattern classification. The EFC valves can be classified in a range that varies between bad to good based on the characteristics yielded as a result of certain inputs. Using fuzzy logic methodology could prove useful to fine tune the acceptable levels of what categorizes a valve to be bad or good, therefore providing ample information before shipment of the EFC valve has been made whether it can remain stable or not within industrial standards.

1.4 About This Thesis

A vast number of methods both in frequency domain and time domain in order to determine the identity and characteristics of the EFC valve were explored in this project. Through observation, it was seen that there were acceptable methods to be used in both domains. Using Bode Diagrams and Step Responses (Chapter 3) proved to give an idea to the identity of the EFC valve, and combining the two methods gave a clue to the order of

the system while maintaining the integrity of the results when compared to one another. The two methods mentioned above have proved to be efficient with process speed, as well as being robust, where the outcomes do not have significant variations, therefore developing a pattern that contributes to the system identification.

Recursive Least Squares (RLS) Estimation (Chapter 3) algorithm was used in discrete time domain in order to give an estimate of the transfer function of the EFC valve. The aforementioned methods that helped narrowing down the order of the EFC valve contributes to RLS procedure as the way it works requires the order of the system being dealt with to be provided. The transfer functions that are outputted as a result of the RLS estimation algorithm varies depending on the nature of the EFC valve; whether it being a failed part, a passed part, or a prototype part. Later on this type of information contributes to the pattern classification (Chapter 4) phase.

The results that were obtained from raw data were simulated in a simulation environment for verification purposes. It is expected that the raw data characteristic curve should be a carbon copy of the simulated characteristic curve. This serves as a tool for reverse verifying that the procedure is in fact doing what it is intended of it, while opening the door to eliminating cross checks between raw data and simulated data.

All these simulation results were verified by experiments conducted at Cummins, Inc. The results proved that this developed test procedure can be used in the fuel systems industry to improve EFC valve performance design.

2 SYSTEM MODELING

An engine governor is a simple device that helps maintain engine speed within the desired limits, regardless of changes in load. A diesel engine governor provides this control by automatically changing the amount of fuel supplied to the engine cylinders. Several types of governors are available to handle many different requirements, such as desired reaction time, speed, and the degree of precision. Governor types include Mechanical; Mechanical / Hydraulic; Mechanical / Electric / Hydraulic, and completely electric governors.

Cummins, Inc. designs and manufactures its own, unique version of a fully electric engine governor: the Electronic Fuel Control (EFC) [1] rotary electrically actuated valve that is used in Cummins diesel engines. It requires no linkage to the throttle shaft; nor does it have any hydraulic component. The EFC valve (actuator), shown in Figure 2.1, is a rotary electrically actuated proportional valve which regulates fuel flow (rail pressure) to the injector fuel supply line in the Cummins Pressure Time (PT) fuel system. The EFC system controls the fuel flow by providing a variable orifice. The size of the orifice is proportional to the duty cycle (pulse width modulated signal) of supplied voltage. Cummins utilizes normally open and normally closed EFC valves.

The governing system consists of the Magnetic Pickup (MPU), which is mounted in the flywheel housing, near the flywheel ring gear, and an Actuator. The Actuator consists of an electromagnetic valve with a fuel port near one end. Depending on the amount of current present in the coil, this port reduces or increases fuel to the injectors. The result is that the engine speed remains within the desired limits, regardless of the changes in load.

This procedure works with the aid of the MPU. The MPU operates on the principal of induced voltage and produces an alternating current (AC) signal that represents the engine speed. The speed signal is transmitted to the Governor Control where it is compared to a preset reference point. If a difference exists between the two signals, the Governor Control will change the current applied to the Actuator Coil. Any change in the Actuator coil results in a change in the strength of an electromagnet. This change causes the Actuator shaft to rotate. The shaft rotation evidently controls the fuel flow to the engine through a rotary valve. This is possible because the Actuator consists of an electromagnetic solenoid valve which, when energized, causes the Actuator shaft to rotate.

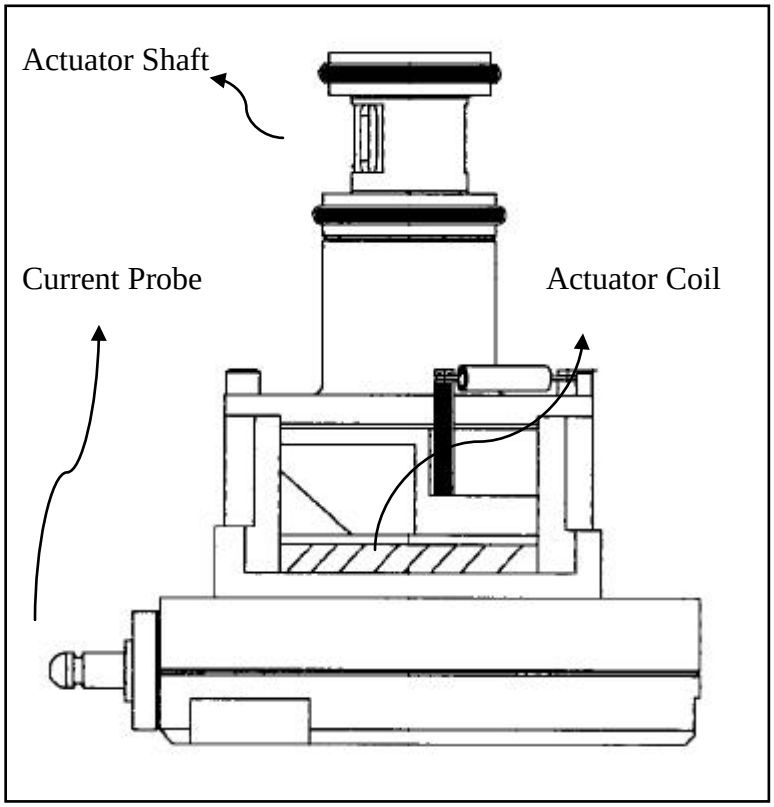

Figure 2.1 EFC components

There are two types of EFC Actuators: Normally Open Actuator and Normally Closed Actuator. In the Normally Open Actuator, the valve is spring loaded to the open position. An increase in the current applied to the coil moves the valve towards the closed position. In the case of the Normally Closed Actuator, the valve is spring loaded to the closed position. An increase in the current applied to the coil moves the valve towards the open position. The valve position in the fuel shaft is demonstrated in Figure 2.2. The alignment can change based on the amount of energy that is fed to the coil. This alignment ranges between no fuel flow and maximum fuel flow. The exact amount depends on the current the coil receives.

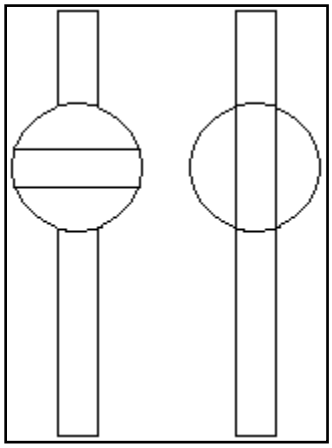

Figure 2.2 Valve alignments in EFC shaft

The rotational design results in a direct relationship between the degree of Actuator shaft rotation and engine HP output. It also results in a direct relationship between angular displacements to the voltage input.

2.1 Development of EFC Valve Dynamic Model

Electromechanical systems are often characterized by the consistency of nonlinear components (e.g. hysteresis, dead time). Components found to be faulty (e.g. stickiness, cracked parts) may cause changes in the characteristics of these systems. Methods which

characterize the nonlinear behavior of systems are well suited to detect such damage. The EFC Actuator is made up of electrical components as well as mechanical components.

2.1.1 EFC Actuator Electrical Subsystem

The electrical part of the EFC is made up of a simple RL circuit to handle the inductive parameters going into the system.

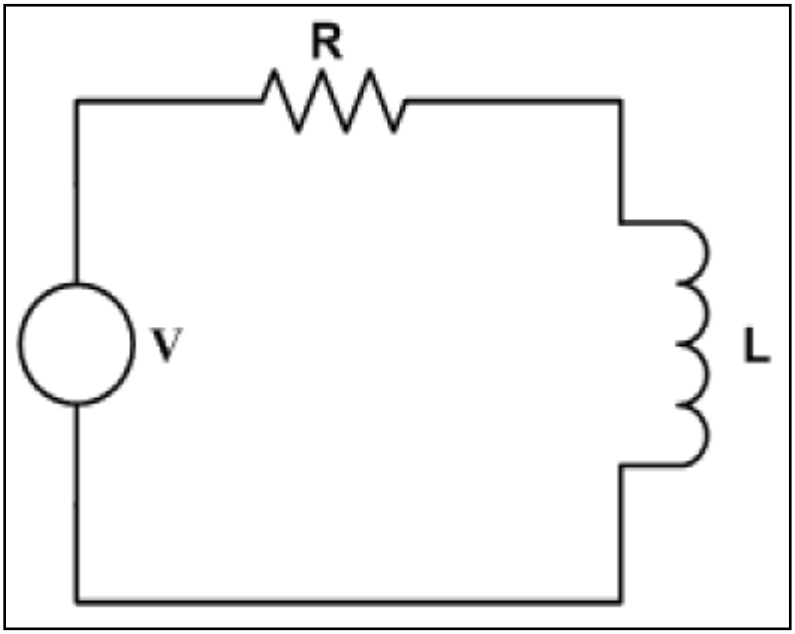

Figure 2.3 Model of the valve solenoid winding

The elements here are Resistance (R), Inductance (L), and a Voltage (V) source, and by the aid of Kirchhoff's Voltage Law and Kirchhoff's Current Law [10] we can obtain the simple RL circuitry equation:

$$V(t) = Ri + L\frac{di}{dt} \tag{2.1}$$

From here it can be observed that the equation is in time domain, but utilizing the Laplace transform [11] can in fact simplify the method of solution. In that case, the equation becomes:

$$V(s) = (R + Ls)I(s) \quad (2.2)$$

Hence this is the model that is solely modeling the electrical side of the EFC Actuator. This formulation will yield to have a common variable with that of the result of the modeling for the mechanical side and therefore will be combined to describe the relationship of electrical components with that of mechanical components.

2.1.2 EFC Actuator Mechanical Subsystem

The other part of the system is comprised of the mechanical components, which is comparatively more complex to the electrical components from a solution stand point. The main body is a cylindrical rotor that is represented in Figure 2.4 [11]:

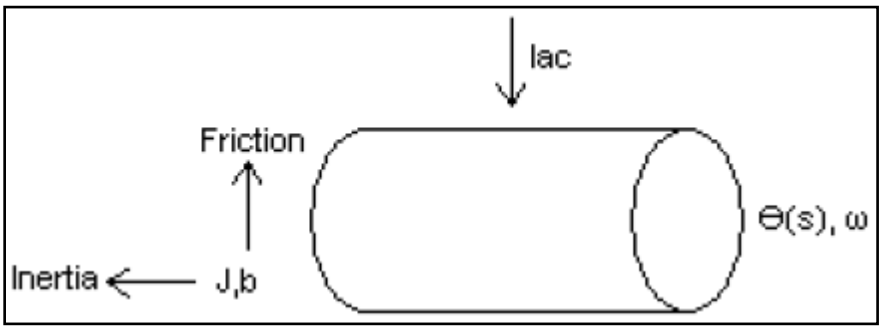

Figure 2.4 Model of the dynamics of the rotary solenoid

Here θ is the angular displacement of the rotor, ω is the angular rate difference, J is inertia, and b is the friction coefficient. It must also be noted that the system has torque (T) delivered to the load as well as a disturbance torque. The disturbance torque is often negligible; therefore the load torque is approximately equal to the torque of the whole rotary solenoid, which can be assumed to be proportional to the current, I. The torque of the rotary solenoid and the load torque for rotating inertia [11] are expressed respectively as:

$$T(s) = KI(s) \quad (2.3)$$

$$T(s) = Js^2\theta(s) + bs\theta(s) \tag{2.4}$$

The two equations combined with (2.2) can be rewritten as:

$$Js^2\theta(s) + bs\theta(s) = KI(s) = K\frac{V(s)}{R+Ls} \tag{2.5}$$

The transfer function relating the input voltage to the angular displacement can then be given by:

$$\frac{\theta(s)}{V(s)} = \frac{K}{\left(Js^2 + bs + k\right)\left(R + Ls\right)} \tag{2.6}$$

The relationship between the angular displacement of the valve and the pressure difference across the valve is highly nonlinear. The nonlinearity is accounted through the involvement of fluid dynamics. Also, the knowledge of hydraulic boundary conditions must be met in order to develop a dynamic model for the relationship of the system. It is assumed that this relationship must be within 2nd order to 6th order, so that all the nonlinearities can be accounted for. In order to be able to model the valve system accurately, methods of linearization must be implemented.

2.2 Linearizing the EFC Valve

With the involvement of nonlinearity, the system became more complex, therefore obtaining the mathematical model became more challenging. In order to be able to analyze the relationships between the system variables and their equations, linearization can help reduce the complexity of the system and help by simplifying the method of solution. By the end of the process we aim to be able to use physical laws to describe the linear equivalent system, and obtain a set of linear differential equations later to be transformed using Laplace Transformation to obtain a solution describing the operation of the system.

The EFC Actuator and its valve can be compared to a hydraulic servo system. Linearization of a hydraulic servo system would reveal clues to the attainability of the linearization for the EFC valve. A hydraulic servo system is essentially a hydraulic power actuator controlled by the use of a pilot valve [12]. With opposing pressure forces acting on it, the pilot valve acts as a balance valve and can control large sums of power outputs, with very little power.

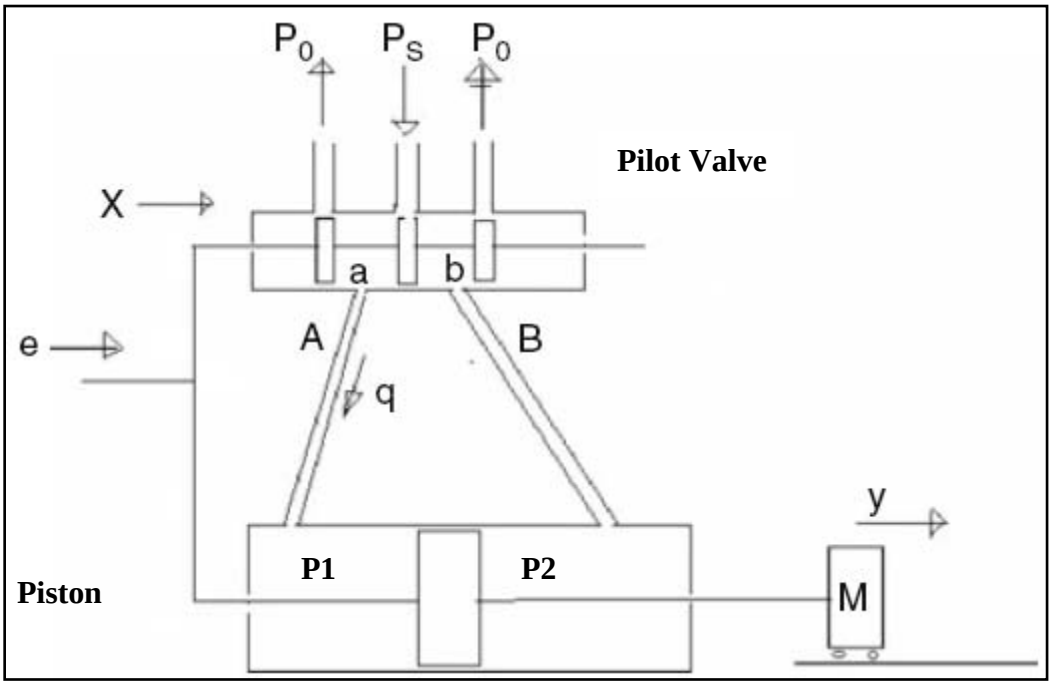

Figure 2.5 Schematic diagram of a hydraulic servomotor

Following an identical design structure with the ports found on the EFC valve, port a, and port b that are shown in Figure 2.5 are made wider than the corresponding valves A and B. This is for the purposes of leakage, an intentional result of a design in order to allow fuel to leak through the valves to act as a coolant, lubricant, and cleaning agent regardless of being in idle state or active state. Leakage contributes to the sensitivity as well as linearity of the system. The variables in the system can be defined as follows:

q = rate of fuel flow

ΔP = P2 – P1 = pressure difference across the piston

x = displacement of pilot valve

From Figure 2.5, it can be observed that q is a function of X and ΔP. To generalize this relationship, the following nonlinear equation can be written among the variables q, x, and ΔP:

$$q = f(x, \Delta P) \tag{2.7}$$

Now this equation needs to be linearized near the normal operating points of $\bar{q}$, $\bar{x}$, and $\Delta\bar{P}$ respectively. The resulting equation:

$$q - \bar{q} = \frac{\partial f}{\partial x}\left(x - \bar{x}\right) + \frac{\partial f}{\partial \Delta P}\left(\Delta P - \Delta\bar{P}\right) \tag{2.8}$$

The partial derivatives must be evaluated at $x = \bar{x}$, $\Delta P = \Delta\bar{P}$, and $\bar{q} = f(\bar{x}, \Delta\bar{P})$. Thus we define

$$K_1 = \left.\frac{\partial f}{\partial x}\right|_{x=\bar{x},\Delta P=\Delta\bar{P}} > 0 \qquad K_2 = -\left.\frac{\partial f}{\partial \Delta P}\right|_{x=\bar{x},\Delta P=\Delta\bar{P}} > 0$$

Note that the as the valve displacement (x) occurs in a positive direction, the fuel flows in a positive direction (positive proportion). For the difference across the piston, when P2 is larger than P1, then fuel flows in a negative direction (negative proportion).

Knowing that normal operating condition corresponds to $\bar{q} = 0$, $\bar{x} = 0$, and $\Delta\bar{P} = 0$, we can rewrite equation (2.8) to yield

$$q = K_1 x - K_2 \Delta P \tag{2.9}$$

This is the rate of fuel to the power cylinder. Looking back at Figure 2.5, it can be observed that the rate of the fuel flow, q, multiplied by dt, is equivalent to the displacement of the piston, dy, multiplied by the area, A, multiplied by the density of the fuel, ρ. This relationship is formulated to be:

$$q dt = A \rho dy \tag{2.10}$$

Keeping in mind that dy/dt pertains to velocity, then for a given flow rate q the larger the piston area A is, the lower the velocity dy/dt becomes. If the piston area A is made smaller, the velocity dy/dt will become higher. This in turn reduces the response time required. Combining equations (2.9) and (2.10) yields

$$\Delta P = \frac{1}{K_2}\left(K_1 x - A\rho\frac{dy}{dt}\right) \tag{2.11}$$

When force developed by the piston, this equates to the multiplication of the difference in pressure ΔP with the piston area A, which would give us

$$A\Delta P = \frac{A}{K_2}\left(K_1 x - A\rho\frac{dy}{dt}\right) \tag{2.12}$$

Should the difference in pressure be high, then the piston area and the density of the fuel become negligible.

When the piston is applied to a load, then mass and friction must be taken into account. The force is developed by the piston AΔP to the mass of the load as well as the friction generated by it. Thus we obtain

$$m\frac{d^2y}{dt^2} + \left(b + \frac{A^2\rho}{K_2}\right)\frac{dy}{dt} = \frac{AK_1}{K_2}x \tag{2.13}$$

Where m is the mass of the applied load, b is the friction coefficient, x is the pilot valve displacement, and y is the piston displacement.

Now we have been able to distinctly establish the assumption of the pilot valve displacement, X, being the input, and the piston displacement, y, being the output. By taking the Laplace Transform and reorganizing equation (2.11) we are able to determine the transfer function, G(s) of the hydraulic servo system:

$$\frac{Y(s)}{X(s)} = \frac{1}{s\left[\left(\frac{mK_2}{AK_1}\right)s + \frac{bK_2}{AK_1} + \frac{A\rho}{K_1}\right]} = \frac{K}{s(Ts+1)} \qquad (2.14)$$

here

$$K = \frac{1}{\frac{bK_2}{AK_1} + \frac{A\rho}{K_1}} \qquad \text{and} \qquad T = \frac{mK_2}{bK_2 + A^2\rho}$$

We have obtained a transfer function of the 2nd order system. If we further speculate that the ratio of the time constant T is negligibly small, or if the time constant T is negligible, than we are left with the simplified transfer function of

$$\frac{Y(s)}{X(s)} = \frac{K}{s}$$

2.3 Relationship of Output and Input

After developing and linearizing the EFC valve, we can use equations (2.6) and (2.11) in order to develop a relationship between the output, pressure (P) and the input, voltage (V). When we were linearizing the EFC valve, we took into account a load on the piston with a displacement of y. In the case of the EFC valve, the load on it is stable; therefore displacement y is equal to zero. Let us recall the equation (2.11),

$$\Delta P = \frac{1}{K_2}\left(K_1 x - A\rho\frac{dy}{dt}\right)$$

and let $\frac{dy}{dt} = 0$,

then we are left with pressure, P as a function of valve displacement, *x*

$$\Delta P = \frac{K_1}{K_2}x \qquad (2.15)$$

Now let us recall equation (2.6),

$$\frac{\theta(s)}{V(s)} = \frac{K}{\left(Js^2 + bs + k\right)\left(R + Ls\right)}$$

The angular displacement, θ can be represented in the form of the pilot valve displacement, *x*, and constant *n (n≠0)*.

$$\theta = nx \tag{2.16}$$

Combining (2.15) and (2.16) allows us to represent pressure, P as a function of angular displacement, θ.

$$P = m\theta \tag{2.17}$$

Where *m (m≠0)* is a constant.

Finally we can revise equation (2.6) with the inclusion of equation (2.17) and we obtain

$$\frac{P(s)}{V(s)} = \frac{K}{m}\frac{1}{\left(Js^2 + bs + k\right)\left(R + Ls\right)} \tag{2.18}$$

Fundamentally, the relationship of the piston displacement, Y(s), to the pilot valve displacement, X(s) relevant to the hydraulic servo system, is the same as the relationship of the angular displacement of the valve, θ(s), to the input voltage, V(s) relevant to the EFC Actuator. This concludes that the linearization of the EFC valve is possible. There are limitations into accurately modeling the EFC valve; the complexity of the systems, and the loss of data in the design of the EFC Actuator itself. The system itself is very complex yet manual fixes exist in the production to account for valve openings and closings. Spring loads are especially manually tweaked with in order to regulate the valves normality conditions; whether being normally open or normally closed. Discharge coefficient of the valve shaft is an important variable that would be considered in the model but the supplier couldn't provide the structural dynamics of the system that would have helped with the calculation of the discharge coefficient.

The EFC Actuator itself has changed three companies since it was first established in the year 1979. Many design documentations as well as design knowledge have been lost over the years and handovers. In order to be able to accurately come up with a mathematical model there are a few more missing variables to be taken into consideration: an estimate of the inertia value, the coefficient of the spring constants, and the damping coefficient of the bearing (friction torque). The values were not able to be calculated because rather than a completed product, it required a product in its infancy phase so that every bit could be individually researched, analyzed, and calculated. The design schematics were not available as well, due to the handovers of design documentations getting lost over the years. Another limiting factor into being able to take a look at the EFC Actuator from the beginning of its production was the fact of the relationship between a supplier (EFC owner) and a customer (Cummins, Inc.). The supplier rightfully so was weary of the potential of losing it business to its direct customer and becoming direct competitors in the market. This hindered the design information in flux.

3 SYSTEM IDENTIFICATION

The dynamic modeling of the EFC valve, which would give a good sense for capturing distinct irregularities between the different types of valves being used, proved to have drawbacks, as indicated in the previous chapter. This chapter discusses how the implementation of system identification helps predict the unknown quantities of the EFC valve in order to help with characterizing the signatures and patterns that they exhibit.

3.1 Identification Experiments

3.1.1 Experimental Setup

The EFC Test Stand is used in a production environment to verify the proper operation of Cummins EFC valves [13]. The EFC Test Stand is capable of accommodating the variety of EFC valves, specifically for the various voltage and normal valve position conditions. As it would be placed onto a pump found on an engine, the EFC valve is placed in a housing on the EFC Test Stand, that lines up the inlets and outlets of each of them so that a continuous stream of fluid can be transferred based on the proportional movement of the orifice that is found on the EFC valve in respect to the duty cycle of a pulse width modulated DC voltage. The fluid that runs through the EFC valve is regulated by a Test Fluid System. The purpose of the Test Fluid System is to maintain the pressure, temperature, and cleanliness of the fluid being tested. Figure 3.1 demonstrates the typical setup of the Test Stand from a frontal view.

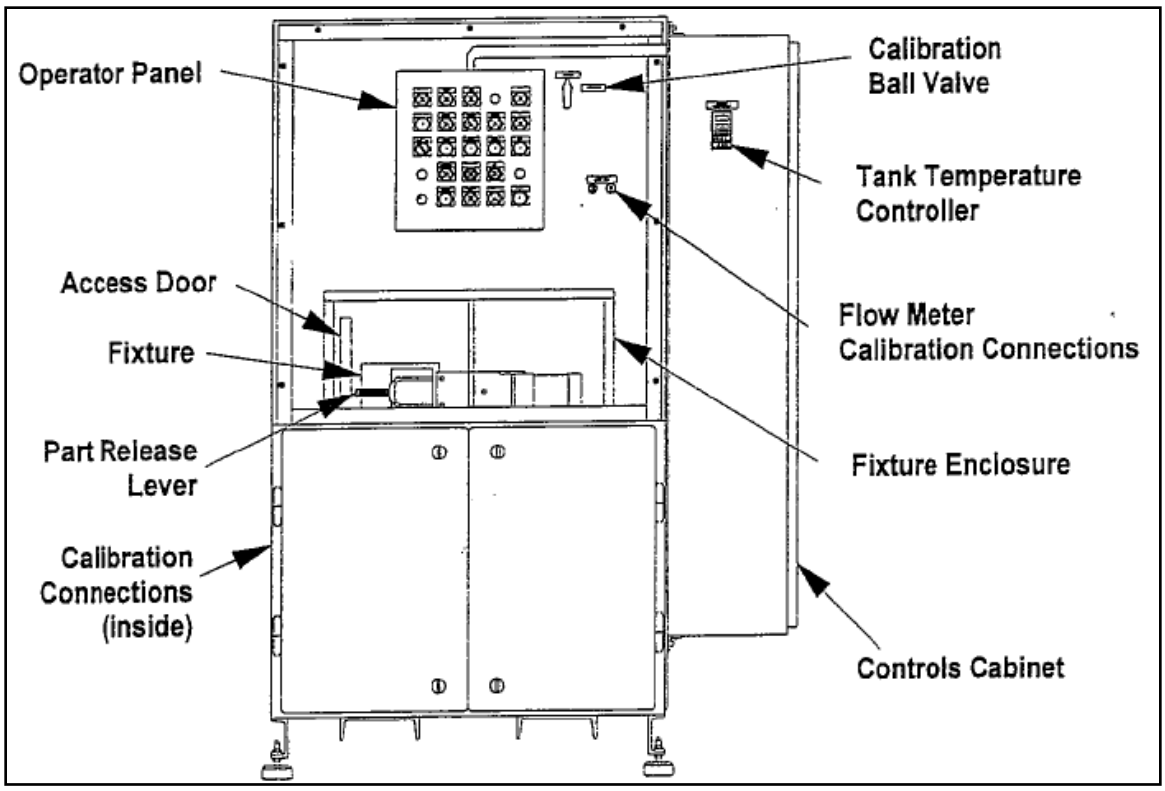

Figure 3.1 Front view of EFC Test Stand

3.1.2 Specifications

In order to be able to achieve accurate testing, the EFC Test Stand must maintain precise parameter specifications that are used to conduct the test. These can be mainly characterized as mechanical, electrical, and hydraulic [14].

3.1.2.1 Mechanical Parameter Specifications

The EFC Actuator placed onto the EFC Test Stand must not have any leakage when subjected to a mean fluid pressure of 300 psig, with peak to peak pressure fluctuations of 50 psig. The EFC Actuator must be capable of withstanding burst pressures of up to 400 psig. The EFC Actuator must also not show any signs of cracking, breaking, or permanently deforming when mounted onto the EFC Test Stand.

3.1.2.2 Electrical Parameter Specifications

The resistance between the two terminal posts (probes) is 2.1 plus/minus 0.4 Ohms for the EFC Actuators categorized as 12 Volts, and 7.2 plus/minus 0.4 Ohms for the EFC Actuators categorized as 24 Volts at 72 plus/minus 1 degrees Fahrenheit. The inductance of the EFC Actuators is less than or equal to 120 milliHenries at 72 plus/minus 2 degrees Fahrenheit. The EFC Actuator must meet all performance requirements after being subjected to 133 percent of the nominal DC voltage of at least 48 hours, while installed in the test housing and filled with fluid. The test housing and the fluid is held at 220 plus/minus 5 degrees Fahrenheit.

3.1.2.3 Hydraulic Parameter Specifications

It should be taken into account that leakage is allowed in the EFC valve to serve in the name of lubricating, cooling down, and cleaning purposes. This leakage should be within the range of 35 cc/min to 125 cc/min with a 220 plus/minus 3 psig pressure going upstream, and 0 plus/minus 3 psig pressure going downstream of the EFC Actuator. The actuation currents required to actuate the EFC valve are given in Figure 3.2.

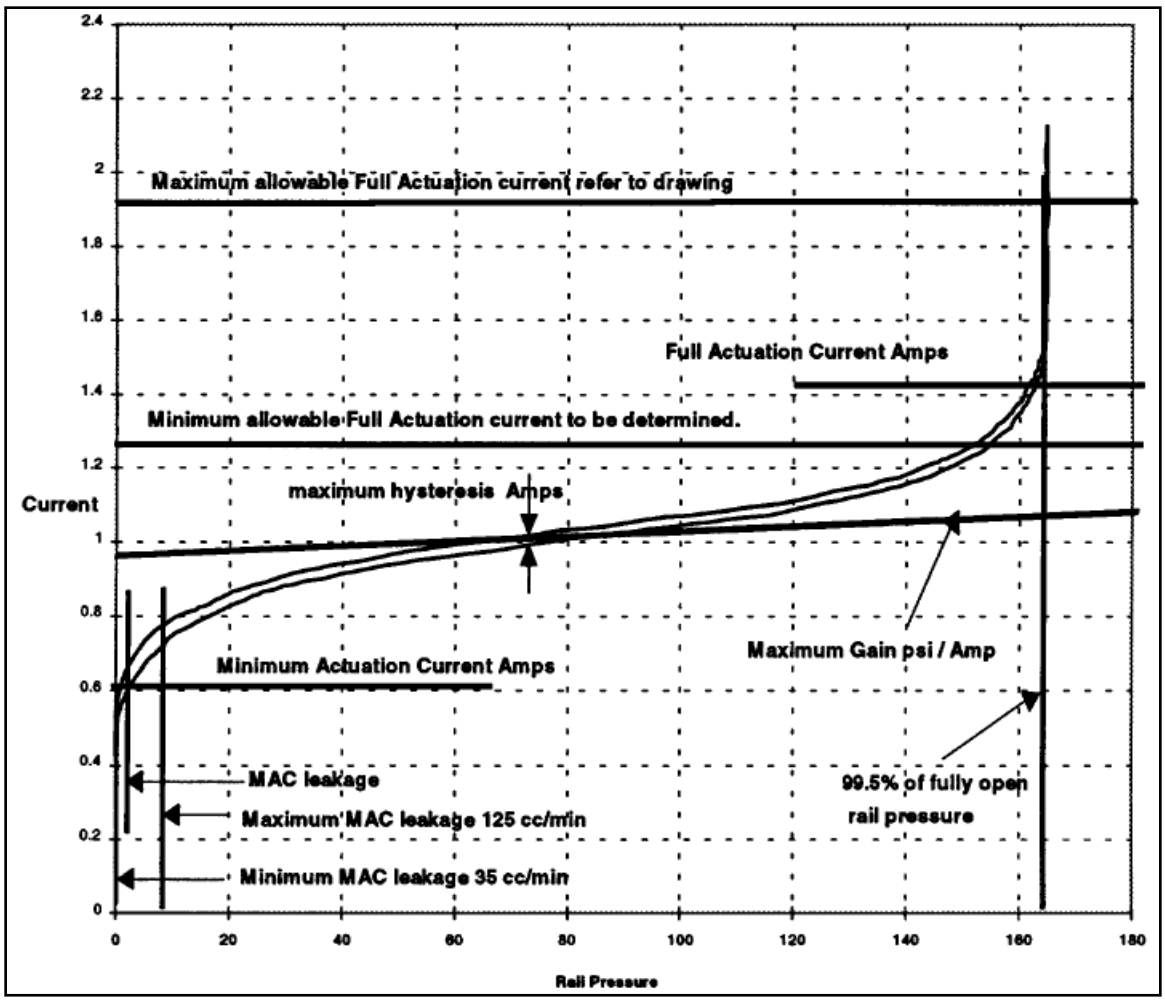

Figure 3.2 Pressure vs. Current of EFC Valve

Once all the specifications have been met, the intended tests could be run. We are able to conduct tests in the frequency domain and the time domain by using frequency response and step response methodology for system identification purposes. The results are provided next.

3.1.3 Experimental Results

3.1.3.1 Frequency Response

For verification purposes, the frequency response test was conducted for different levels of fluid pressure. The pressure levels reached are as follows: 19-21 psig which is achieved with a low amplitude signal sweep, 20-140 psig which is achieved with a medium amplitude signal sweep, 133-147 psig which is achieved with a high amplitude signal sweep.

Figures 3.3 and 3.4 show the Bode Diagrams that have resulted from low amplitude sweep, for various categories of EFC Valves. These categories are return valve, prototype valve, and good valve. Figure 3.3 shows the experimental results for the normalized gain of the EFC Valves, and Figure 3.4 shows the experimental results for the phase lag of the EFC Valves. For both plots, it can be seen that the three types of EFC Valves demonstrate different signatures on the characteristic curves. In the normalized gain figure, the valve categorized as return starts decaying earliest, followed by the valve categorized as prototype, and lastly the valve categorized as good. As expected, the same pattern repeats itself for the phases that are associated with the normalized gains.

The signatures become more evident for medium amplitude signal sweeps, as can be seen in Figures 3.5 and 3.6. The decaying of the valves first occurs for the return valve, followed by the prototype valve, and finally the good valve. However, when we introduce higher amplitude signal sweeps, this pattern becomes random as can been seen from Figures 3.7 and 3.8.

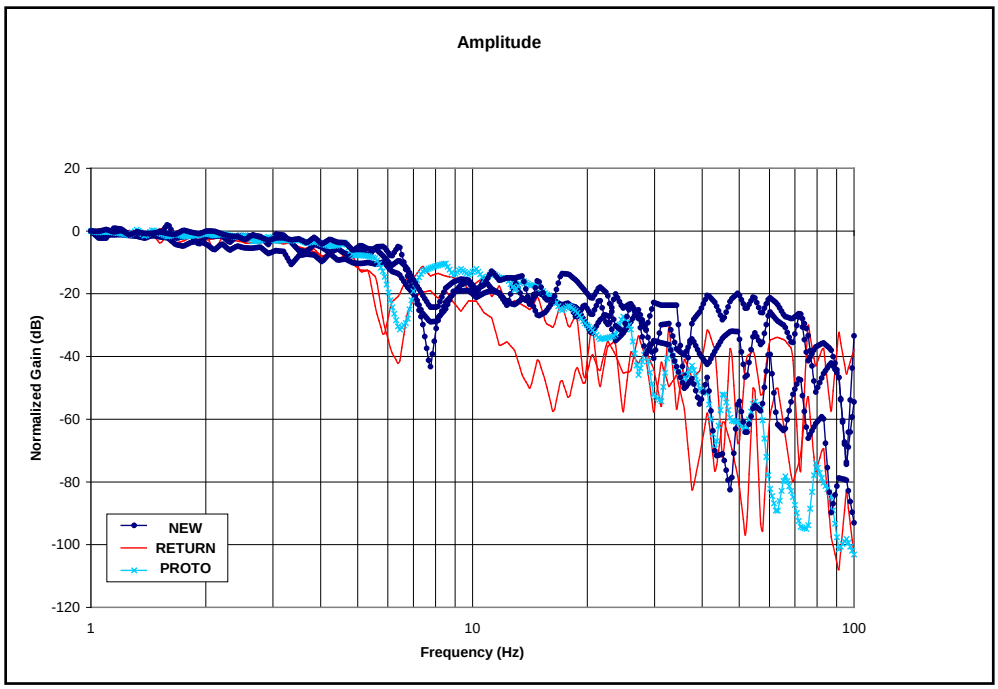

Figure 3.3 Normalized gains of the EFC Valves with low amplitude

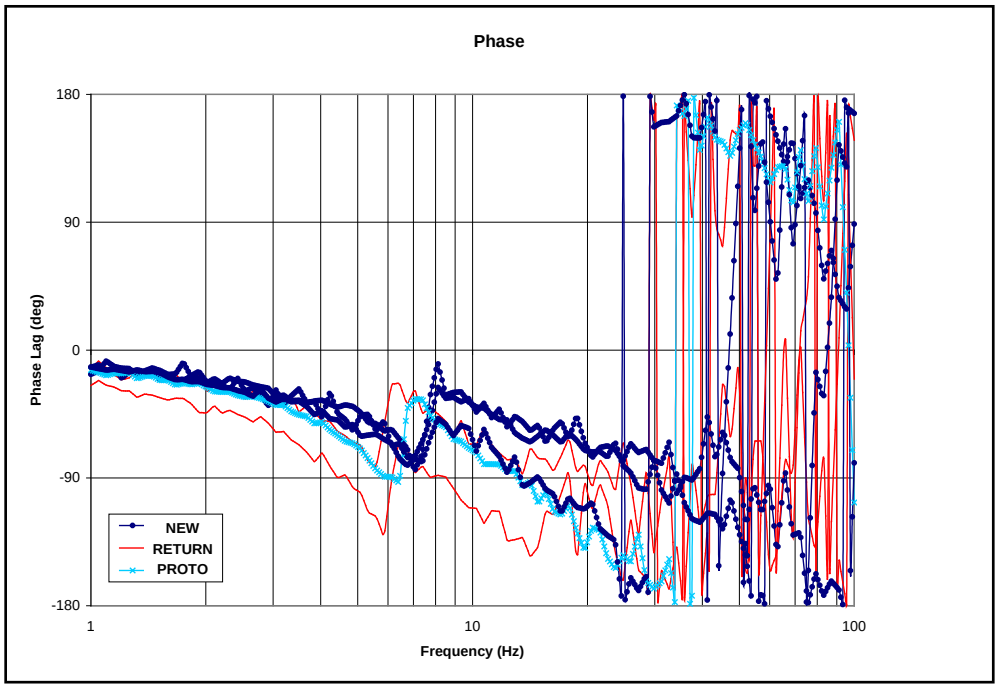

Figure 3.4 Phase lags of the EFC Valves with low amplitude

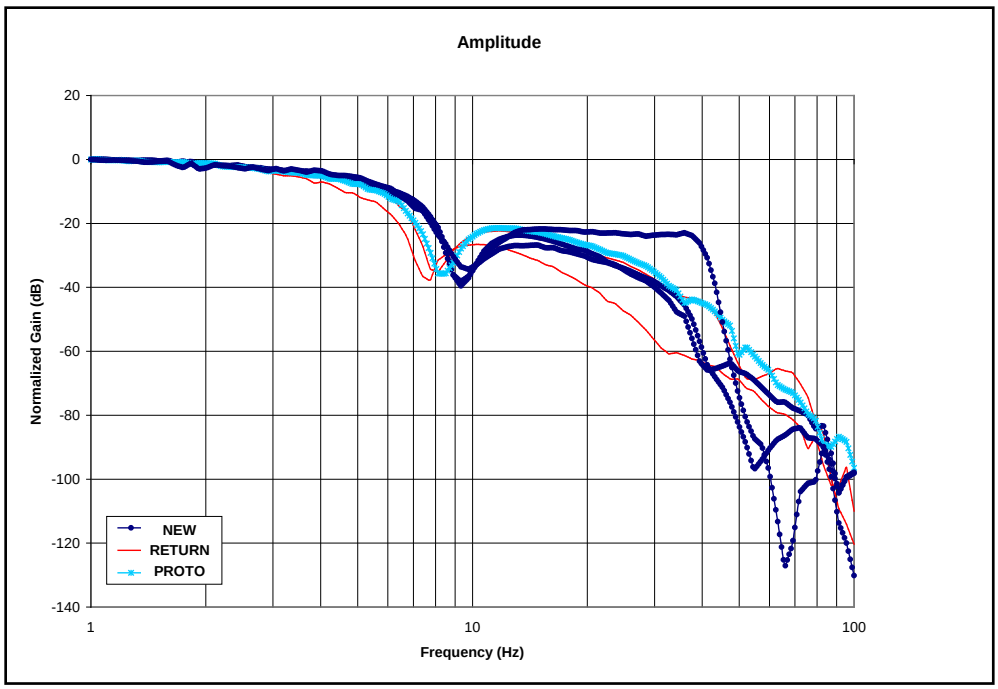

Figure 3.5 Normalized gains of the EFC Valves with medium amplitude

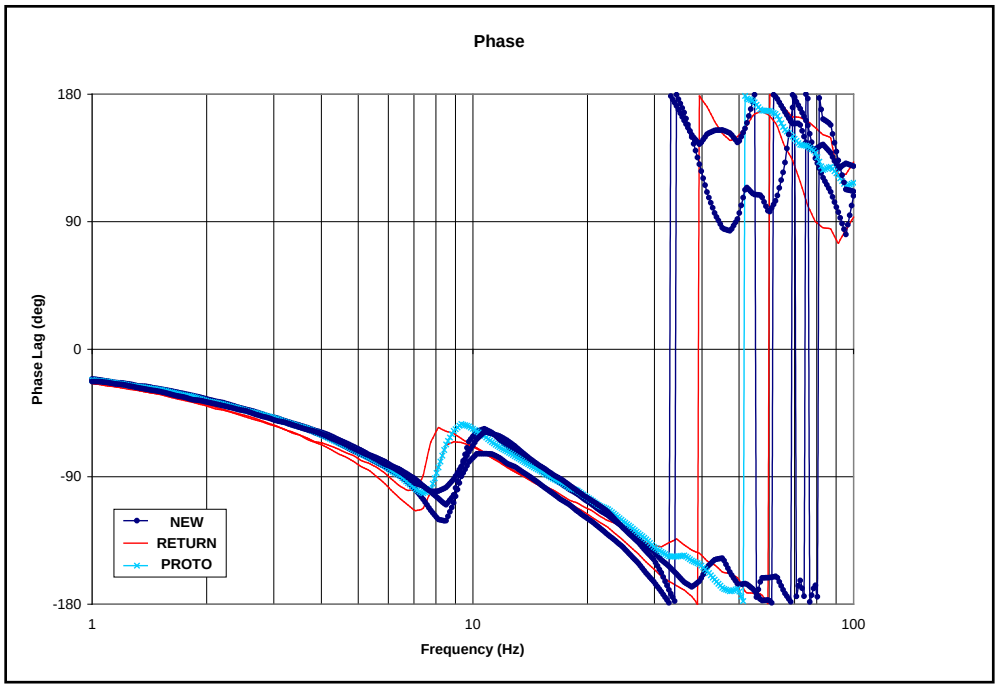

Figure 3.6 Phase lags of the EFC Valves with medium amplitude

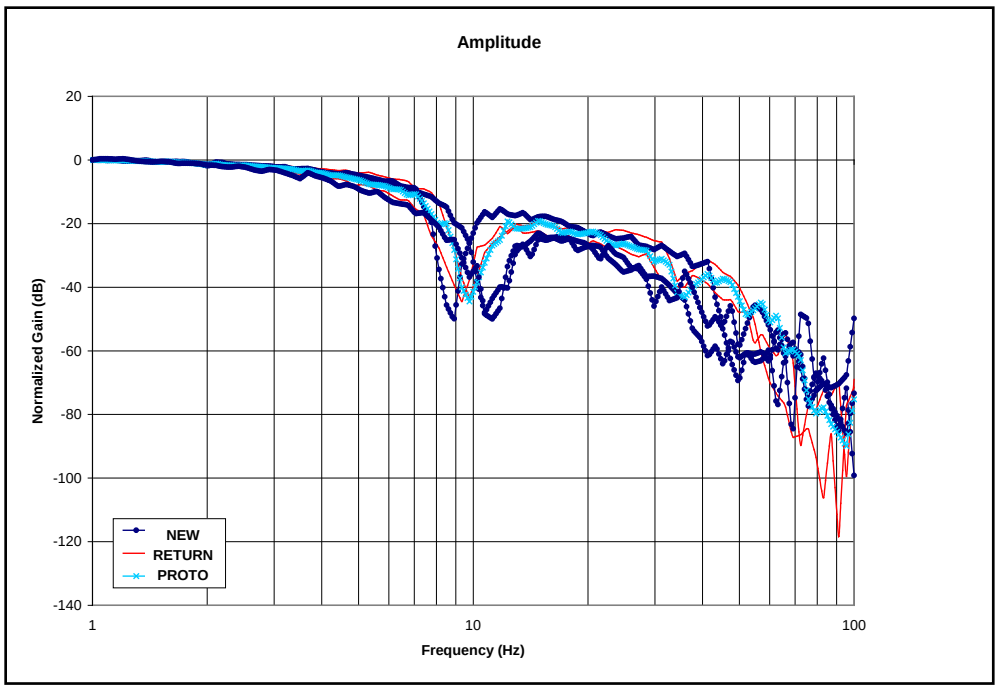

Figure 3.7 Normalized gains of the EFC Valves with high amplitude

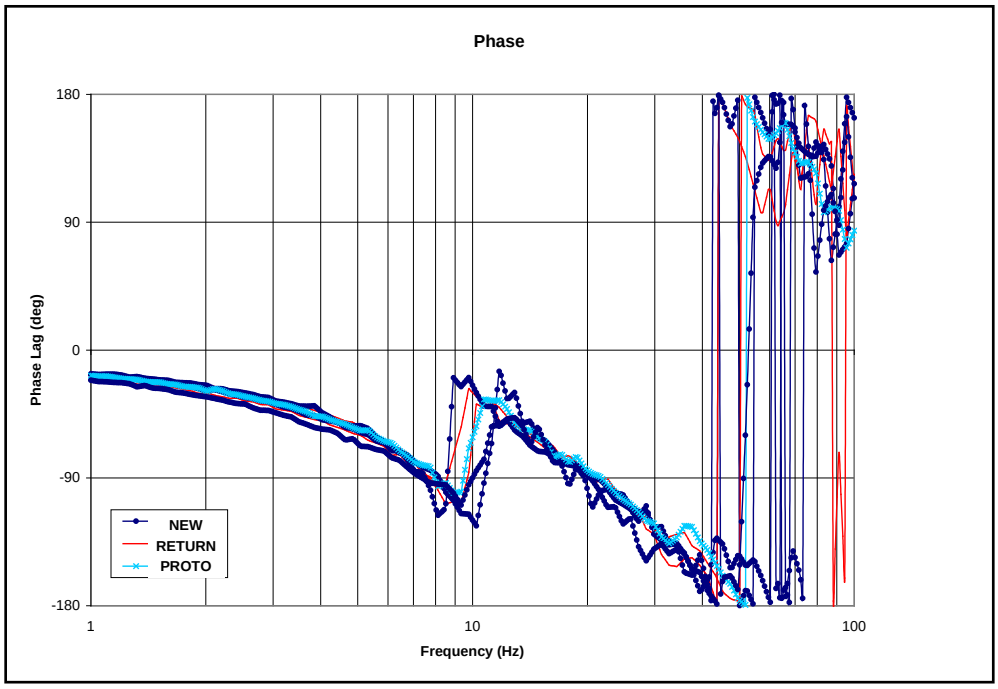

Figure 3.8 Phase lags of the EFC Valves with high amplitude

3.1.3.2 Step Response

The step response test was conducted for different levels of mean maximum fluid pressure. The pressure levels reached are as follows: 3.1 psig which is achieved with a current input of 1.2 Amps, 26 psig which is achieved with a current input of 1.4 Amps, 120 psig which is achieved with a current input of 1.6 Amps, 160 psig which is achieved with a current input of 1.8 Amps, and 210 psig which is achieved with a current input of 2.0 Amps.

The notations X_R and X_S represent real data and simulated data respectively. The real data is what we have obtained through data acquisition of the step response, and the simulated data was obtained through the procedure of Recursive Least Square (RLS) method which is addressed in Section 3.2.2.1. The purpose of including X_S on the responses helps the observation between characteristic differences of the EFC valves; it has no effect towards the functionality of the step responses.

Figures 3.9 and 3.10 show the step response diagrams that have resulted from current input signal of 1.2 Amps, for various categories of EFC Valves. These categories are return valve, and good valve. Figure 3.9 shows the experimental result for the returned EFC Valve, and Figure 3.10 shows the experimental result for the good EFC Valve. From both plots, it can be seen that the two types of EFC Valves demonstrate slightly different signatures on the characteristic curves. In the return valve figure, the rising time of the response is slower compared to the rising time of the response for the good valve.

The signatures become more evident as the current inputs increase in amplitude, as can be seen in Figures 3.11 thru 3.18. The difference in rising times of the valves becomes more evident; where from the response of the return valve we can observe that

more time is necessary to rise. Another difference in signatures is at the settling portion of the response. The settling portion corresponding to the return valve, lands far away from the simulation, while the settling portion corresponding to the good valve, lands flat on or within close proximity. These variations are seen in Figures 3.17 and 3.18.

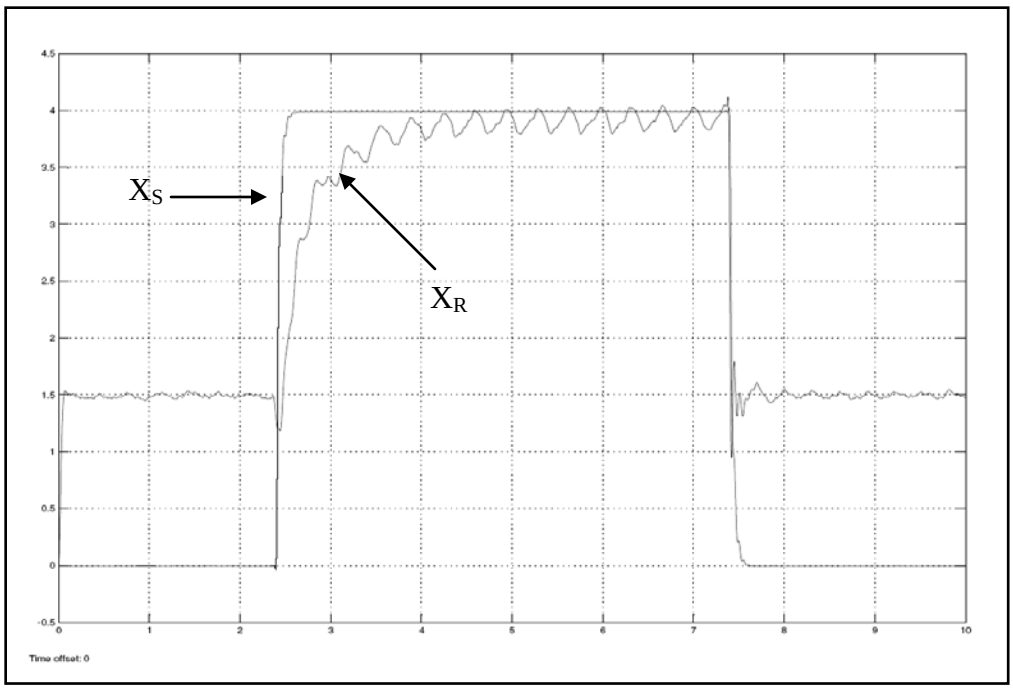

Figure 3.9 Return EFC Valve with 1.2 Amps current input

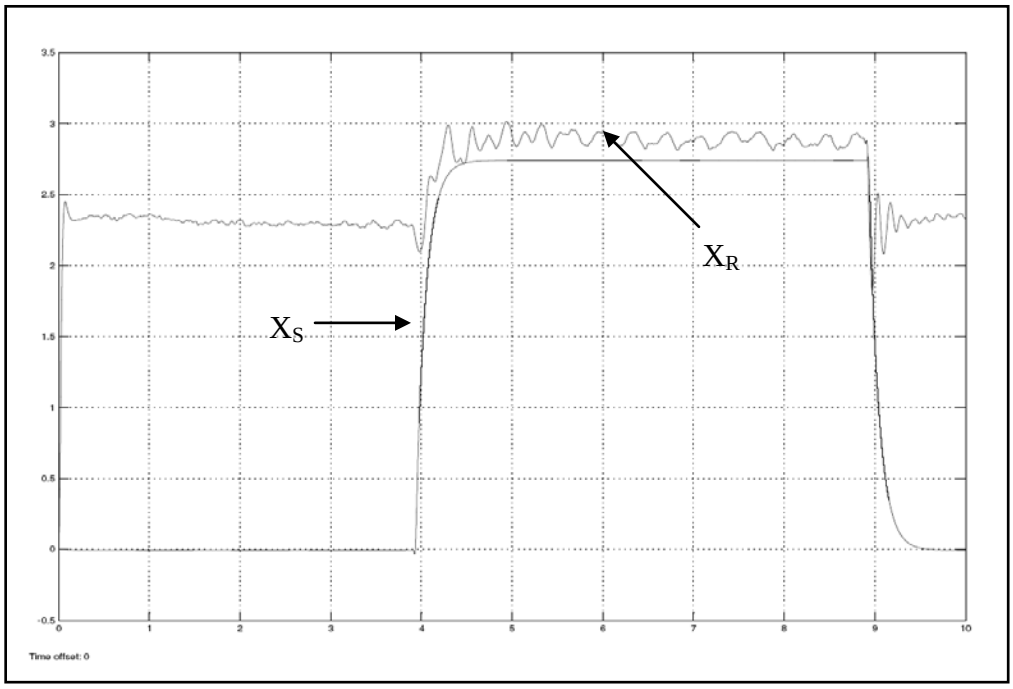

Figure 3.10 Good EFC Valve with 1.2 Amps current input

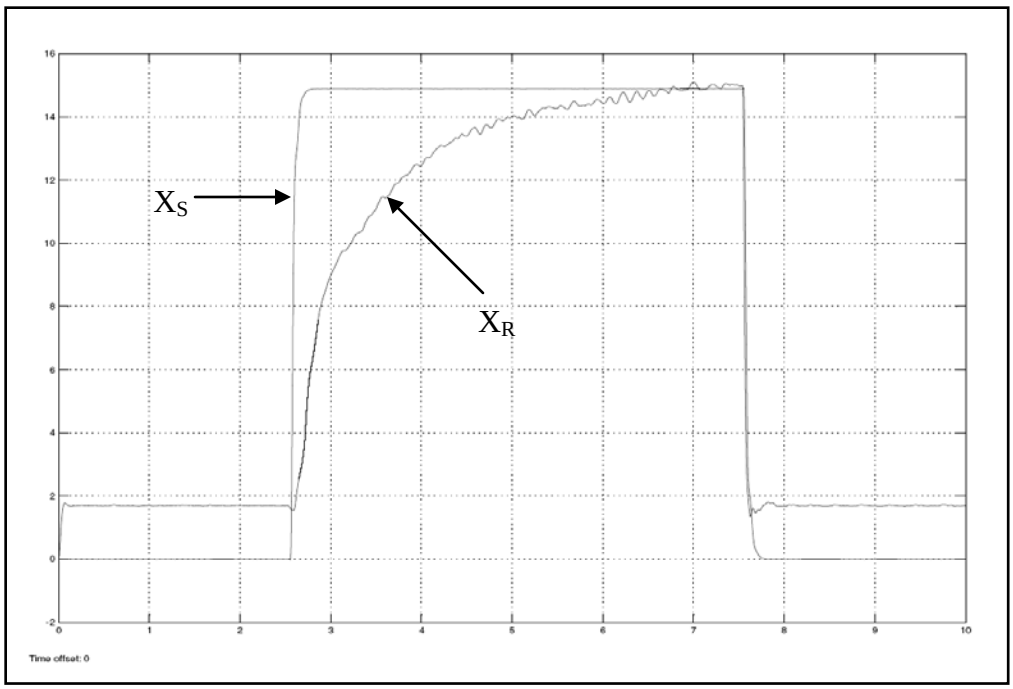

Figure 3.11 Return EFC Valve with 1.4 Amps current input

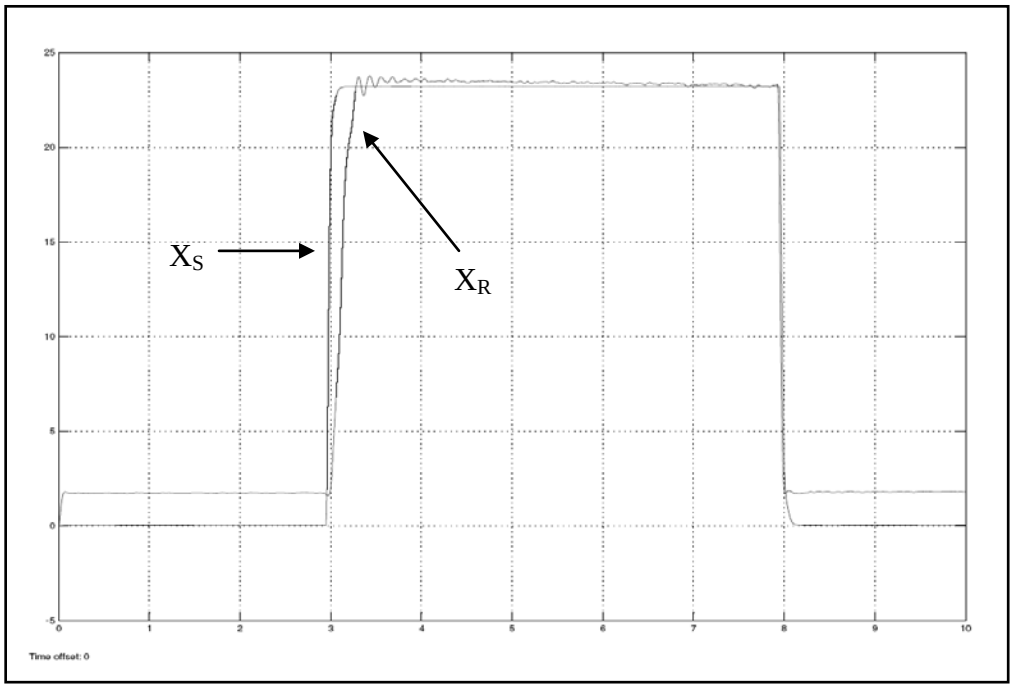

Figure 3.12 Good EFC Valve with 1.4 Amps current input

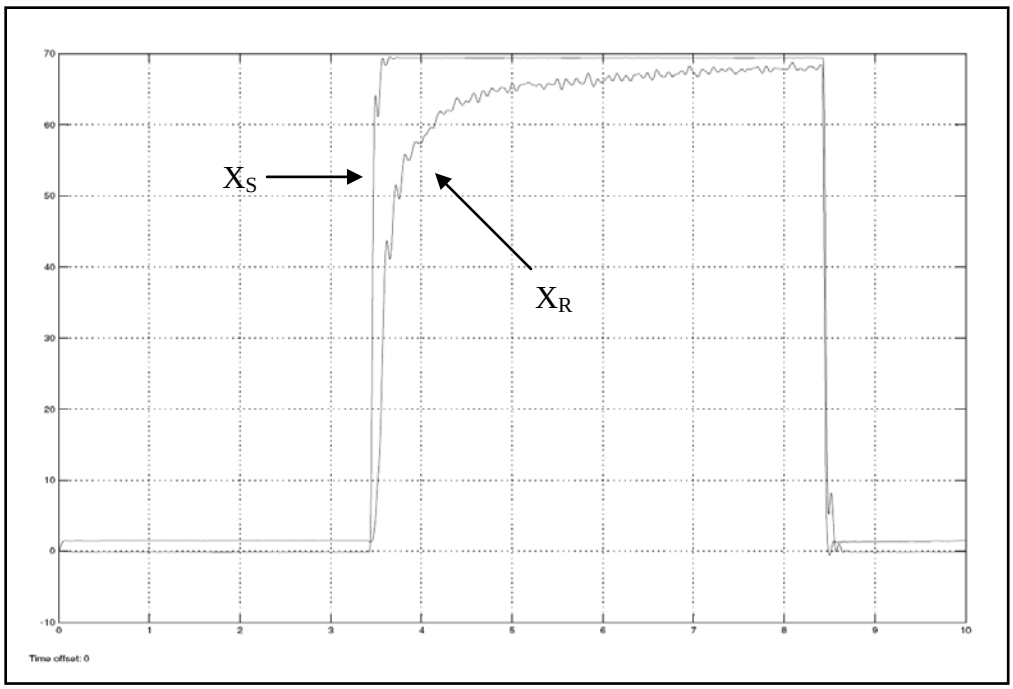

Figure 3.13 Return EFC Valve with 1.6 Amps current input

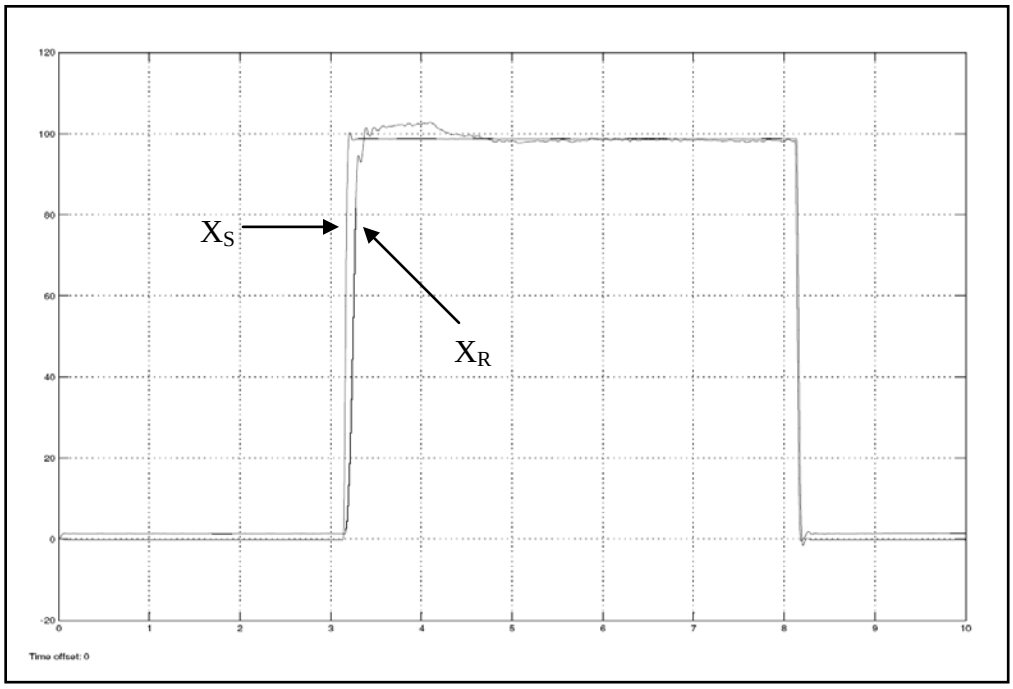

Figure 3.14 Good EFC Valve with 1.6 Amps current input

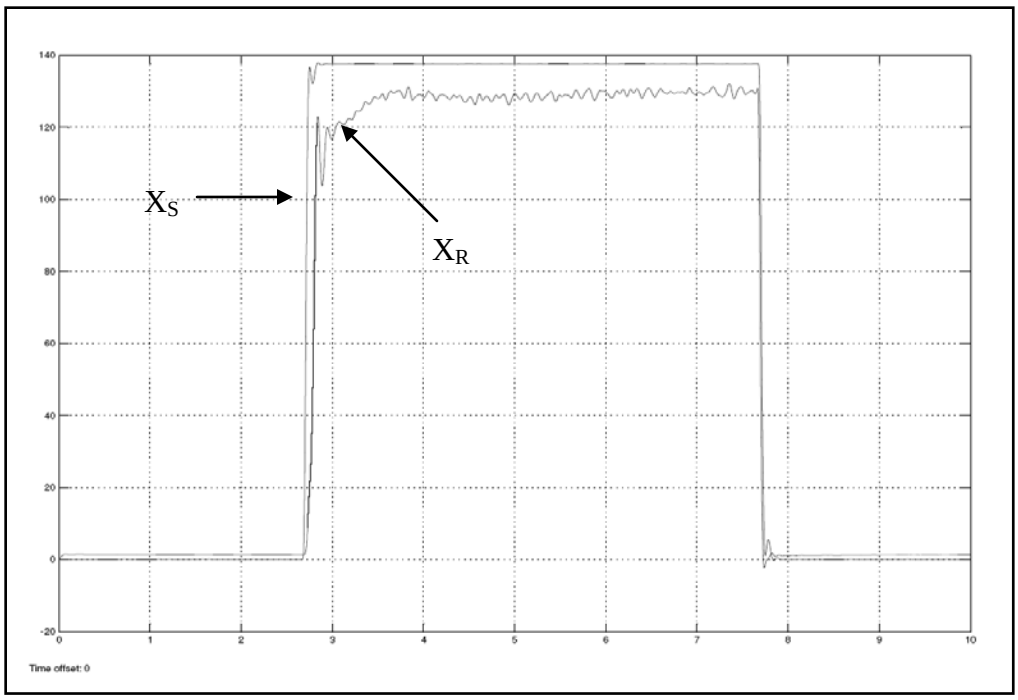

Figure 3.15 Return EFC Valve with 1.8 Amps current input

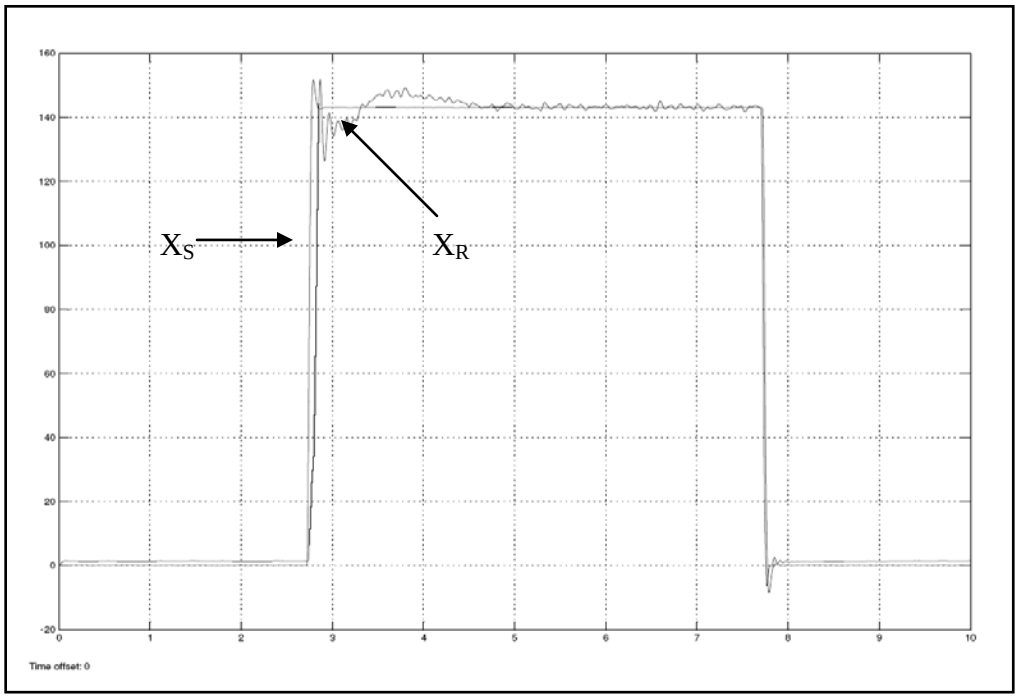

Figure 3.16 Good EFC Valve with 1.8 Amps current input

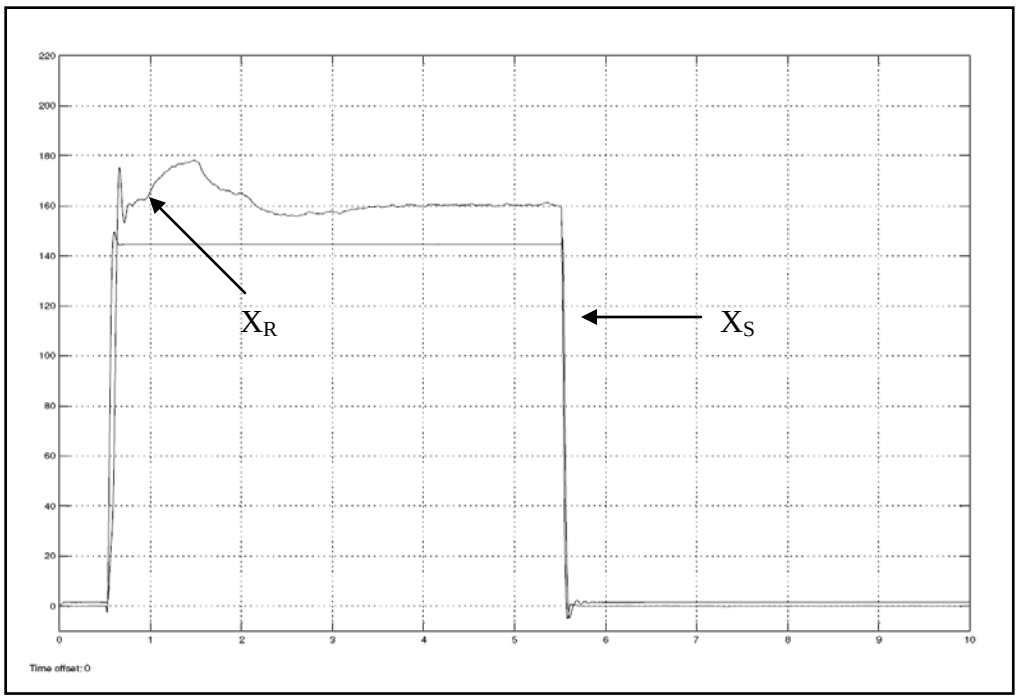

Figure 3.17 Return EFC Valve with 2.0 Amps current input

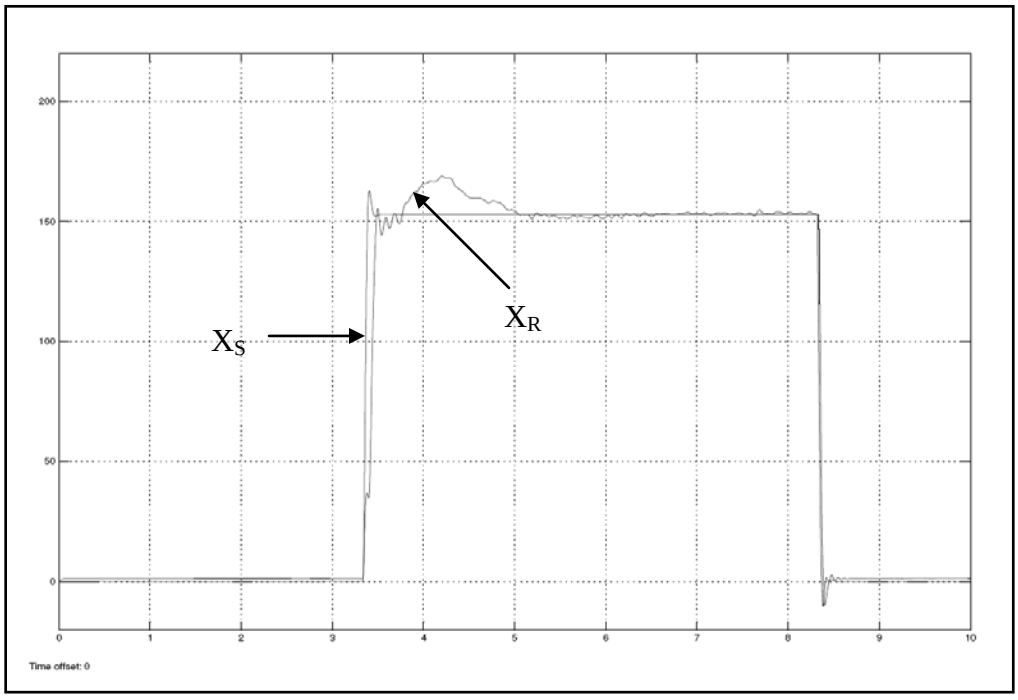

Figure 3.18 Good EFC Valve with 2.0 Amps current input

3.2 Transfer Function Estimation

The results of the previous section demonstrate that there are in fact significant differences between a return EFC Valve and a good EFC Valve. However, the identity of the EFC Valve has still not been established. This section looks into the various methods used in identification, in order to identify the EFC Valve. Methods for frequency domain as well as time domain are demonstrated.

3.2.1 Frequency Domain Method

Frequency domain identification techniques were first chosen for estimation of the transfer function of the EFC Valve because of the benefits that came along with it: the ease of reducing the noise (noisy frequency lines being eliminated), reduction of the amount of data when compared to time domain data, the ease of removing the DC offset errors found in the input and output signals, no need to initially estimate the state of the system, and the ease of removing the output drift [15].

The Bode Diagrams of the EFC Valves that were constructed as a result of the frequency response give a good indication to the characteristics of the transfer function associated with the EFC valve; an educated estimation of the transfer functions [16] can be made by analyzing the characteristics of the curves, such as the slope of the asymptotes on the normalized gain plots, corner frequencies, and phase conditions. It is important to be able to estimate the poles and zeros of a transfer function, and this can be done through minimization and estimation. Once these are determined the order of the system becomes important as well. From observation, the system appears to have a range from five to nine. This can be accounted to the fluid dynamics of the system as well as the electrical and mechanical side. Only after the consideration of these variables can we start with the structuring the model of the EFC Valve. The algorithm developed by Santos and Carvalho has been followed, where the minimization of error has been the focal point.

$$V = \frac{1}{2}\sum_{k=1}^{N}\left[\ln\left|Y\left(j\varpi_k\right)\right| - \ln\left|\frac{B\left(j\varpi_k\right)}{A\left(j\varpi_k\right)}\right|\right]^2 \tag{3.1}$$

Here, $Y\left(j\varpi_k\right), k = 1,...,N$ denotes the Frequency Response set, and B/A denotes our estimated transfer function.

3.2.1.1 Model Structure

Let us assume that we will have a transfer function of the following nature [16]:

$$G(s) = \frac{\prod_{i=1}^{n_z}\left[\left(s/-z_j\right)+1\right]}{\prod_{i=1}^{n_p}\left[\left(s/-p_j\right)+1\right]} \tag{3.2}$$

$p_j \in R,\ i = 1,...,n_p$

$z_j \in R,\ i = 1,...,n_z$

To this transfer function, the corresponding Bode plot is proportional to

$$LmG(x) = \sum_{i=1}^{n_p+n_z} t_i\left(x_i - \frac{1}{2}\ln e^{2x} + e^{2x_i}\right) = \sum_{i=1}^{n_p+n_z} Lmg_i\left(x, x_i, t_i\right) \tag{3.3}$$

$x = \ln(\omega),\ x_1 \le x_2,...,x_{n_p+n_z}$

$x_i = \ln\left|p_j\right| \Rightarrow t_j = 1,\ j = 1,...,n_p$

$x_i = \ln\left|z_j\right| \Rightarrow t_j = -1,\ j = 1,...,n_z$

And the asymptote:

$$asst_i\left(x, x_i, t_i\right) = \begin{cases} 0 & \Leftarrow x \le x_i \\ -t_i\left(x - x_i\right) & \Leftarrow x \ge x_i \end{cases} \tag{3.4}$$

By computing the difference of (3.3) and (3.2) we can understand what the magnitude of the Bode plots, the normalized gain plots for our case, depend on.

$$asst_i(x, x_i, t_i) - Lmg_i(x, x_i, t_i) = \begin{cases} 0.5t_j \ln\left(1 + e^{2(x-x_i)}\right) & \Leftarrow x \le x_i \\ 0.5t_j \ln\left(1 + e^{-2(x-x_i)}\right) & \Leftarrow x \ge x_i \end{cases} \quad (3.5)$$

It depends on the distance ($x-x_i$); the magnitude is largest when $x=x_i$ and approaches zero when $(x - x_i) \to \pm\infty$. This must be taken into consideration as the transfer function estimation is being established along with the other factors mentioned earlier on.

3.2.1.2 Asymptotic Approximation to the Bode Diagram

With the assumption of using a continuous set of measurements in $[x_{min}, x_{max}]$, our estimates can be refined through minimization to the following format:

$$J(\bar{\theta}) = \frac{1}{2}\int_{x_{min}}^{x_{max}} \left[LmY(x) - assy(x, \overline{\theta, r})\right]^2 dx$$
$$assy(x, \overline{\theta, r}) = \sum_{i=1}^{n} assy_i\left((x, \overline{x_i}, t_i)\right) \quad (3.6)$$

where $n = n_p + n_z$. In the case of either all the poles or all the zeros being equal to zero transfer functions with poles and zeros sufficiently far apart, the minimum of $J(\bar{\theta})$ will lie in a region where V is convex, therefore containing the minimum of V. This information about the poles and zeros therefore demands attention when it comes to minimizing (3.1).

3.2.1.3 Estimations

The transfer functions of the EFC Valves have been estimated by taking into consideration the contributing factors mentioned earlier. Once the transfer function estimation is satisfactory, the Bode plots of the transfer functions are simulated, and then superimposed onto the original Bode plots that were generated earlier. This is mainly a

trial and error approach, where the results get better after continuous ‘tune ups’. Figures 3.19 through 3.21 represent the Bode plots with the simulated results for three categories of EFC Valves: prototype valve, good valve, and return valve.

The estimated transfer function is of the ninth order. The Bode plot of this transfer function has been created and superimposed on the original Bode plot of the EFC valve. The following figures represent the result of the different types of EFC valves, followed by their estimated transfer functions respectively.

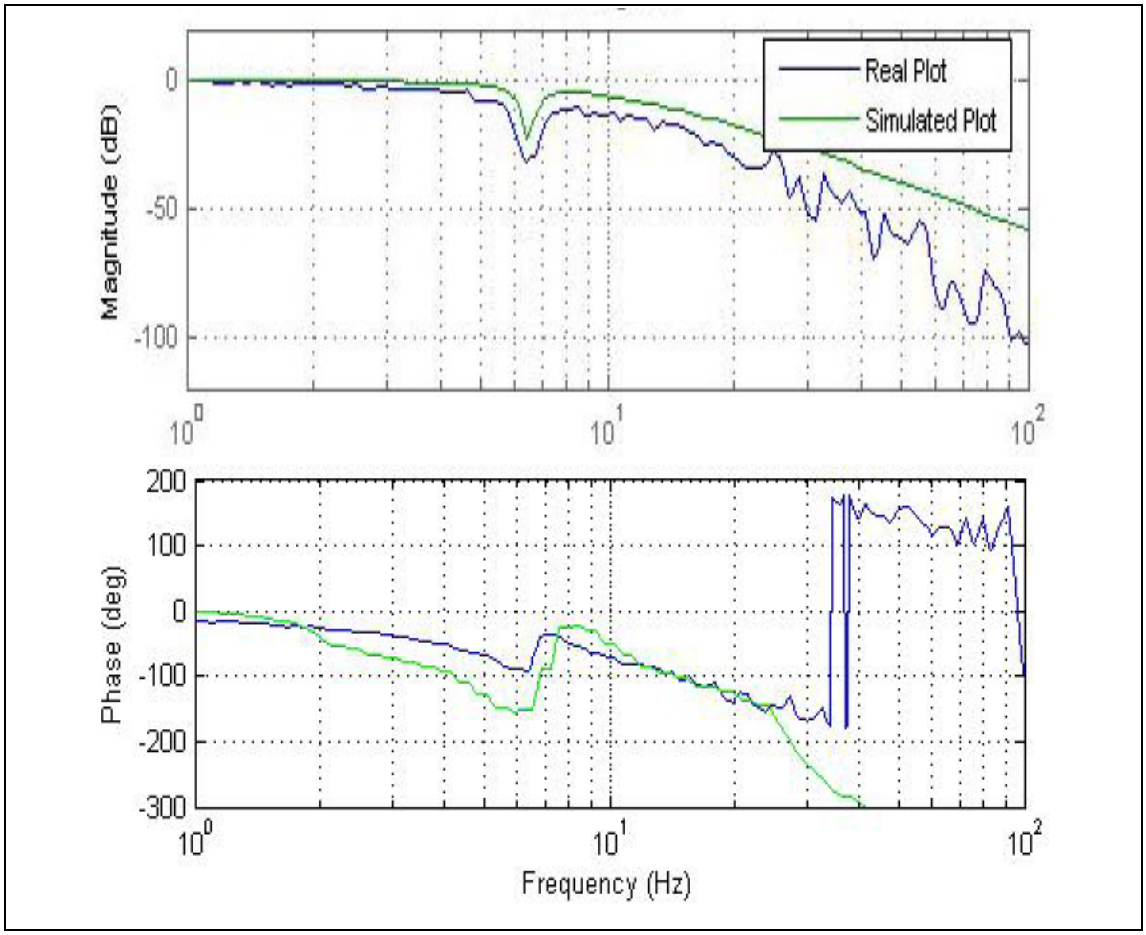

Figure 3.19 Prototype valve simulations

The estimated transfer function is:

$$G(s) = \frac{\left(\frac{s}{0.5}+12.5\right)\left(\frac{s^2}{6.5s^2}+\frac{2\zeta s}{6.5}+1\right)^2 kdc}{\left(\frac{s}{12.25}+12.5\right)\left(\frac{s^2}{6.5^2}+\frac{2\zeta s}{6.5}+1\right)^2\left(\frac{s^2}{9.75^2}+\frac{2\zeta s}{9.75}+1\right)^2}$$

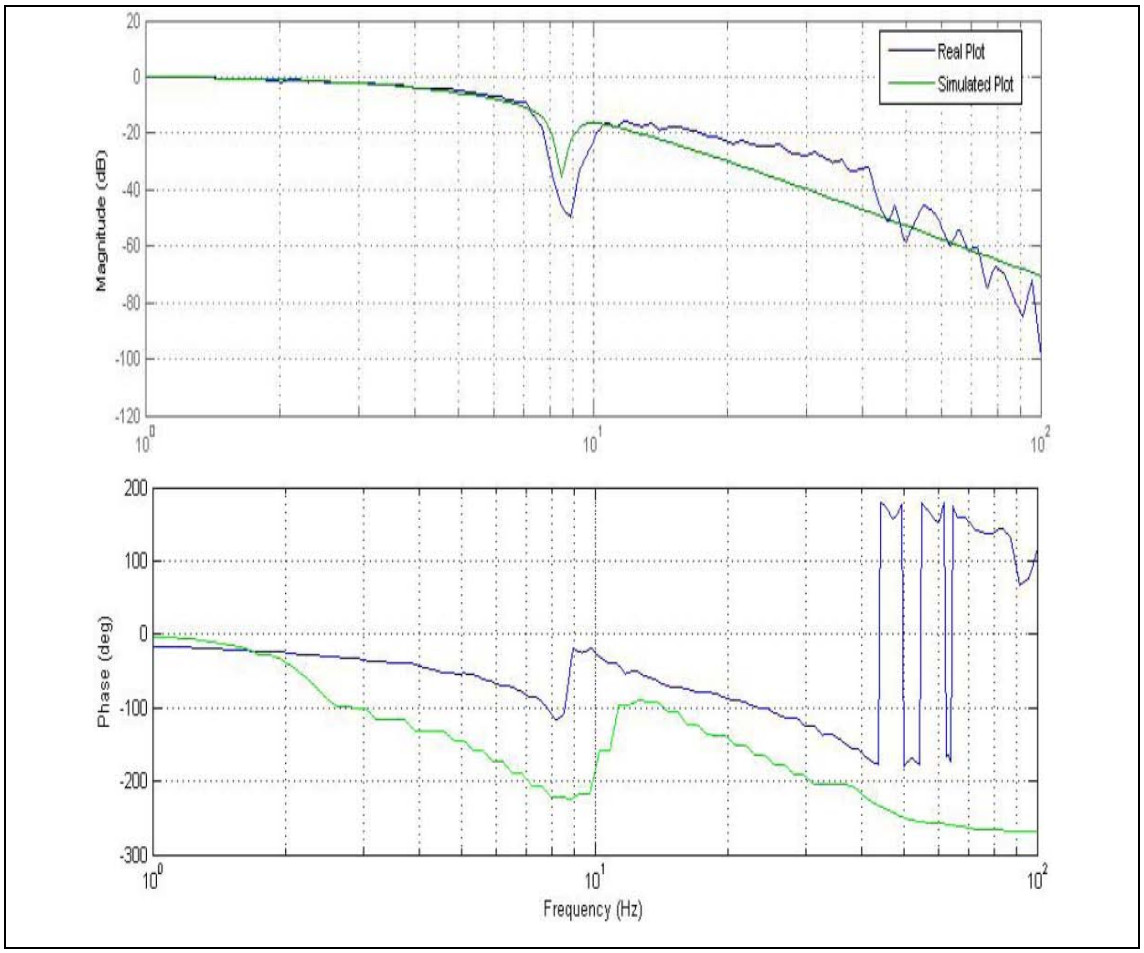

Figure 3.20 Good valve simulations

The estimated transfer function is:

$$G(s)=\frac{\left(\frac{s}{1.05}+12.5\right)\left(\frac{s^2}{8.5s^2}+\frac{2\zeta s}{8.5}+1\right)^2 kdc}{\left(\frac{s}{1.75}+3.5\right)\left(\frac{s^2}{8.5^2}+\frac{2\zeta s}{8.5}+1\right)^2\left(\frac{s}{10}+1\right)^2}$$

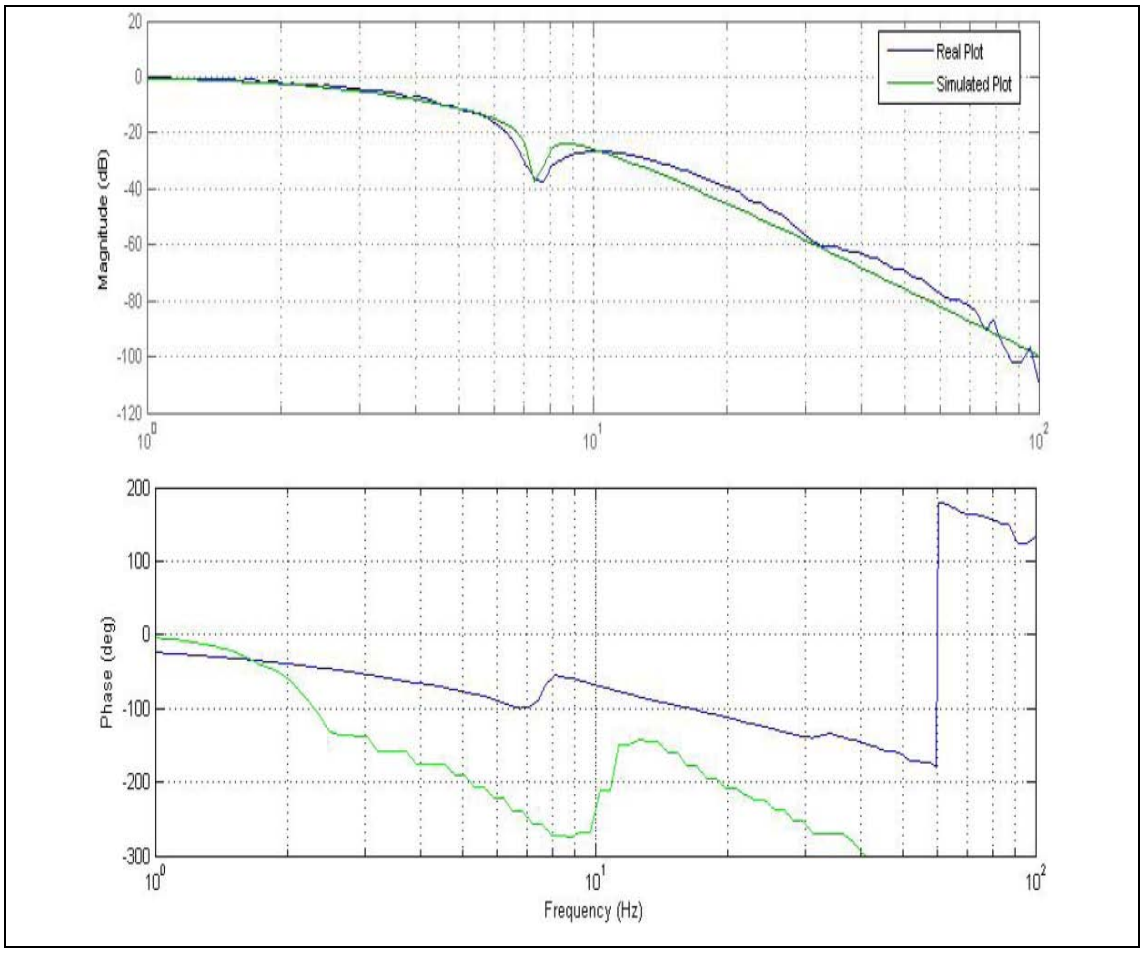

Figure 3.21 Return valve simulations

The estimated transfer function is:

$$G(s) = \frac{\left(\frac{s}{1.05}+12.5\right)\left(\frac{s^2}{7.5s^2}+\frac{2\zeta s}{7.5}+1\right)^2 kdc}{\left(\frac{s}{1.05}+3.5\right)\left(\frac{s^2}{7.5^2}+\frac{2\zeta s}{7.5}+1\right)^2\left(\frac{s}{10}+1\right)^3}$$

The disadvantage of this approach is that it is a complex and cumbersome method. The identified transfer function is of eighth or ninth order. The transfer function can be derived to the necessary structure, but the coefficients are small and sensitive

enough to make significant impact on the simulated plots. This causes the trial and error method to take a long time to show satisfactory results. As the trial progresses, the error minimizes, and the results get better.

3.2.2 Time Domain

As the complexity of systems increase, the effectiveness of the frequency domain system identification methodology decreases. Time domain methodology proves to be a simple and robust approach for identifying systems of a complex nature and it can contain the data in boundary conditions provided by the user.

The pressure responses of the EFC Valves that were constructed as a result of the step response already proved effective results to their characteristic signatures as mentioned earlier. The transfer function of the EFC Valves can be estimated by identifying the model parameters using a given set of data with the help of a system identification tool already proven effective in this field. This method could be conducted in an offline manner; however, proceeding online, as new data points become available proves to be more effective. The raw data that has been acquired is analyzed and then utilized for the purposes of estimating the transfer function using the Recursive Least Squares (RLS) algorithm. [7, 8, 9].

3.2.2.1 Recursive Least Squares Algorithm

For the purpose of indentifying the model parameters of the EFC Valve, the RLS algorithm is based on the following model. [7, 8, 9].

$$\begin{aligned}\Delta y(t) = &-\hat{a}_1\Delta y(t-1) - \hat{a}_2\Delta y(t-2) + \hat{b}_0\Delta u(t-k) + b_1\Delta u(t-k-1) \\ &+ \hat{b}_2\Delta u(t-k-2) + \hat{b}_3\Delta u(t-k-3) + \xi(t) + \hat{c}_1\xi(t-1)\end{aligned} \tag{3.7}$$

Assume $\hat{c}_1$ to be zero (since it is the coefficient of correlated noise), and (3.7) becomes

$$\Delta y(t) = \Psi^T(t-1)\hat{\theta}(t-1) + \varepsilon(t) \tag{3.8}$$

$\varepsilon(t)$ represents an error that is assumed to be statistically independent of the inputs and outputs. Ψ^T and $\hat{\theta}$ are the regression vector and parameter vector respectively, and are defined as

$$\Psi^T(t-1) = \begin{bmatrix} -\Delta y(t-1), -\Delta y(t-2), \Delta u(t-k), \Delta u(t-k-1), \\ \Delta u(t-k-2), \Delta u(t-k-3) \end{bmatrix} \tag{3.9}$$

$$\hat{\theta}(t-1) = \left[\hat{a}_1, \hat{a}_2, \hat{b}_0, \hat{b}_1, \hat{b}_2, \hat{b}_3\right] \tag{3.10}$$

where

$$\Delta y(t-1) = y(t-1) - y(t-2) \tag{3.11}$$

The parameters making up the transfer function are estimated by finding estimates of $\hat{\theta}$ of the unknown parameter θ that will minimize the loss function:

$$J[\theta] = \sum_{i=1}^{N} \lambda^{N-1}\left[\Psi^T(t-1)\theta - \Delta y(t)\right]^2 \tag{3.12}$$

Here λ is a weighing factor in the range of $0 < \lambda \leq 1$ that weighs new data more heavily than old data.

The Recursive Least Squares algorithm used to estimate the transfer functions of the EFC Valves is expressed as follows:

$$\hat{\theta}(t) = \hat{\theta}(t-1) + K(t)\left[\Delta y(t) - \Delta\hat{y}(t)\right] \tag{3.13}$$

$$K(t) = \frac{P(t-1)\Psi(t-1)}{\lambda + \Psi^T(t-1)P(t-1)\Psi(t-1)} \tag{3.14}$$

$$P(t) = \frac{1}{\lambda}\left[1 - K(t)\Psi^T(t-1)\right]P(t-1) \tag{3.15}$$

P is the covariance matrix of the estimation error of the parameter estimates, $\Delta\hat{y}(t)$ follows from (3.8) for $\varepsilon(t) = 0$, and K(t) is the Kalman filter gain, which multiplies the prediction error in order to portray the correction term for the model parameter vector. Equation (3.13) requires an initial estimate of the parameter vector $\hat{\theta}$, and equations (3.14) and (3.15) require an initial estimate of P(0).

3.2.2.2 Recursive Least Squares Application Example

What this algorithm is basically doing is obtaining parameters from data vectors, of both input and output signals. These are the parameters that make up the transfer function of the EFC Valves. This example will provide a better understanding of how the RLS estimation algorithm works. A known transfer function is used for demonstration purposes. The output vector is regenerated using the known transfer function only to be used to identify the specified transfer function for validation.

Two types of responses have been tested: Sinusoidal Response and Step Response. One method is utilizing a sinusoidal signal as an input, and the other is using a step signal as an input; both of the signals are used as the input vector that is used in the RLS algorithm. The results from both responses are compared with one another in order to determine which method provides a better estimation.

To illustrate, let us consider the following arbitrary transfer function in the discrete time domain:

$$G(z) = \frac{0.001 + z^{-2}}{1 + 0.3z^{-2} - 0.5z^{-4}}$$

The RLS estimation algorithm was coded in MATLAB script and the input / output data was generated using standard differential equations. The input and output data are then fed into the RLS estimation algorithm to estimate the transfer functions'

parameter coefficients. The estimated coefficients and actual coefficients are then compared for accuracy. Then parameter vectors that are used are:

A = [1 0 0.3 0 -0.5]

B = [0.001 0 1]

We expect to see the resulting estimated parameters at the end of the RLS estimation algorithm to be close in value to vectors A and B.

The first input is the sinusoidal signal and it generates the following output:

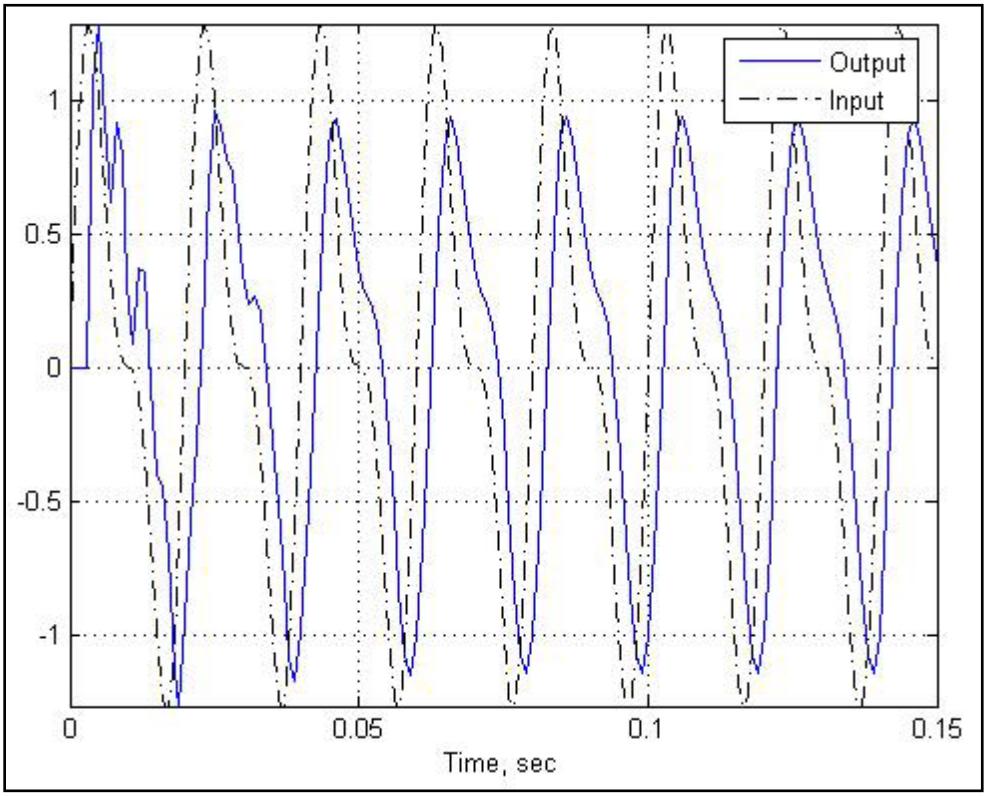

Figure 3.22 Sinusoidal Response

The parameter coefficients that have been estimated:

$\hat{A}$ = [1.000 -0.0578 0.3069 -0.0221 -0.4623]

$\hat{B}$ = [-0.0105 0.0488 0.9186]

To clarify the information above, $\hat{A}$ and $\hat{B}$ are the estimates generated of the real parameters vectors, A and B respectively.

Table 3.1 Results from sinusoidal response

Real Parameters		**Estimated Parameters**	
A	**B**	**A^**	**B^**
1	0.001	1	-0.0105
0	0	-0.0578	0.0488
0.3	1	0.3069	0.9186
0		-0.0221	
-0.5		-0.4623	

As evident from the table, the estimated results are close, but not exact. Next, the step signal is inputted, and the following output is generated.

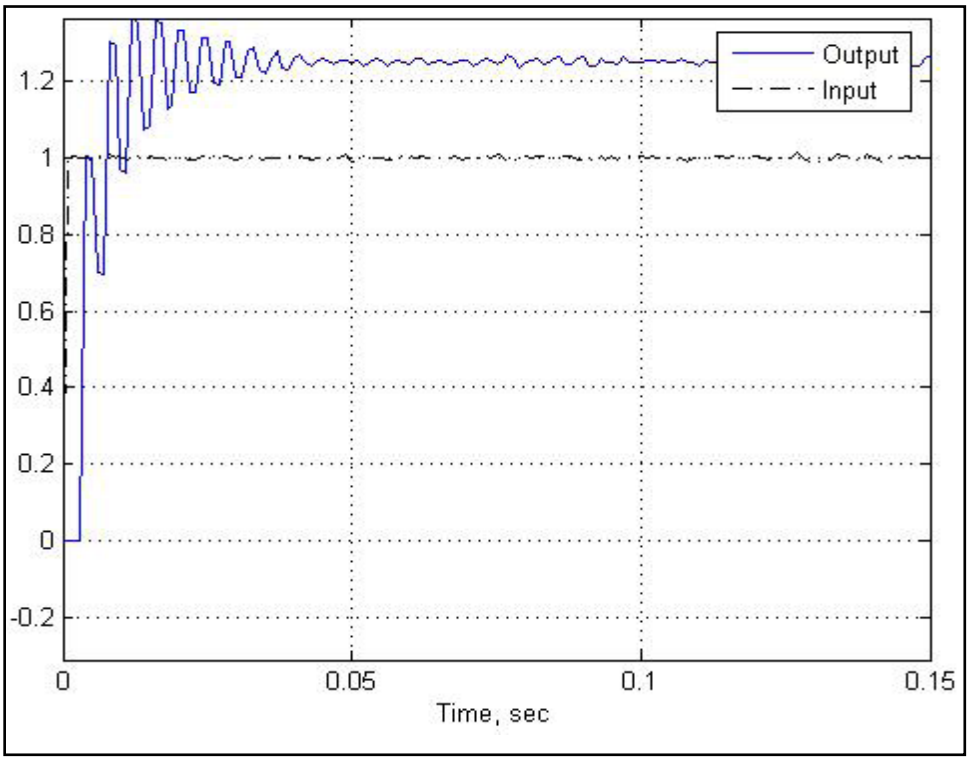

Figure 3.23 Step Response

The parameter coefficients that have been estimated:

$\hat{A}$ = [1.000 -0.0000 0.3000 -0.0000 -0.5000]

$\hat{B}$ = [-0.0010 -0.0000 1.0000]

To clarify the information above, $\hat{A}$ and $\hat{B}$ are the estimates generated of the real parameters vectors, A and B respectively.

Table 3.2 Results from step response

Real Parameters		**Estimated Parameters**	
A	**B**	**$\hat{A}$**	**$\hat{B}$**
1	0.001	1	0.001
0	0	0	0
0.3	1	0.3	1
0		0	
-0.5		-0.5	

It can clearly be seen that the step response estimates parameters with a lot more confidence and accuracy. In the case, the estimated parameters are exactly the same as the real parameters.

3.2.2.3 Estimations

The transfer functions of the EFC Valves have been estimated by taking into consideration the contributing factors mentioned earlier. The raw data that was acquired earlier is run through the RLS estimation algorithm. As was approximated earlier if the frequency domain analysis, the order of the system is around nine. Below are some examples of the estimated transfer functions for various categories of EFC Valves.

Transfer function estimate for a prototype EFC Valve:

$$G(z) = \frac{-0.001 + 0.001z^{-1} + 0.001z^{-4}}{1 - 4.679z^{-1} + 9.469z^{-2} - 11.31z^{-3} + 9.644z^{-4} - 6.813z^{-5} + 3.919z^{-6} - 1.493z^{-7}}$$

Transfer function estimate for a good EFC Valve:

$$G(z) = \frac{-0.001 + 0.002z^{-3} + 0.05z^{-5}}{1 - 2.501z^{-1} + 2.209z^{-2} - 1z^{-3} + 0.464z^{-4} - 0.208z^{-5} + 0.078z^{-6} - 0.007z^{-7}}$$

Transfer function estimate for a return EFC Valve:

$$G(z) = \frac{0.001z^{-3} + 0.001z^{-4}}{1 - 5.058z^{-1} + 11.2z^{-2} - 14.6z^{-3} + 12.93z^{-4} - 8.539z^{-5} + 4.261^{-6} - 1.416z^{-7}}$$

When we take a look at the estimated transfer functions, there is no conclusive evidence to the way the different types of EFC Valves have been modeled. The coefficients are too minute between each other to observe a distinct difference in characteristics. Furthermore, the coefficients don't appear to be maintaining a certain pattern within each category of EFC Valve; the results are random at best. The role of leakage can be a contributing factor to the discrepancy, as it causes for the response to never have zero value throughout the entirety of the input. In other words, when the input is zero, the output is a low value, rather than being zero as well. Another contributing factor is the "stickiness" of the EFC Valve, which causes the EFC Valve trouble when opening and closing, rendering the procedures' stability useless.

These transfer functions come in handy when they go through a step response, and come up with a simulated response, X_S (Refer to Section 3.1.3.2). The simulated response is then superimposed onto the real response, X_R at which point comparisons can be made between characteristic signatures between the EFC valves. The data from the simulated response, X_S is also a key element for the procedure of pattern classification using fuzzy logic approach, and is explained in the following chapter (Section 4.1.2).

4 PATTERN CLASSIFICATION

From the results of the system identification, each valve demonstrated to maintain a distinct difference in characteristics. These characteristics eventually evolved into certain patterns depending on the type of valve experimented. This chapter discusses how the implementation of fuzzy logic helps classify the different types of valves based on their patterns.

4.1 Fuzzy Logic

4.1.1 Basic Concepts of Fuzzy System

Introduced in 1965 by Lotfi Zadeh, fuzzy logic means approximate reasoning, information granulation, computing with words and so on [17]. Different than classical logic, where sets are determined to be true or false based on the numeric assignments of the values of {0, 1}, fuzzy logic allows for the sets to have degrees of memberships. Like classical logic, in fuzzy logic, 0.0 represents classical falsity, 1.0 represents classical truth. However, intermediate degrees of uncertainty can be assigned to all the values between 0 and 1 to deal with ambiguity and vagueness.

In other words, fuzziness deals with the notion of perception depending on the way we look at things. For instance, a car travelling 55 mph can be considered fast by individual X, while a car travelling 45 mph can be also considered fast for another individual Y. Based on these two definitions, it can be seen that no unique definition is

provided for the variable of “fast”. Degrees of memberships can be assigned in order to eradicate the vagueness of perception that arises from one individual to another. More specifically for the topic of this thesis, an EFC valves’ type can be determined as they differ from one another in a manner of being very stable, stable, unstable, and very unstable. These terms are of course fuzzy statements that pertain to the fact that the EFC valve is good or bad.

Fuzzy logic systems develop human reasoning into an algorithm or program in order to make a decision or a control system. It is made up of fuzzy sets, which is the conversion of crisp sets, which is the original set from the acquired data. Fuzzy sets are used to represent uncertainty, and are used to make inferences in fuzzy logic [18]. The degree of the fuzzy set memberships must be represented by membership functions which are commonly triangular, Gaussian, and trapezoidal functions.

The manner of flow of the procedure of fuzzy logic systems is to start off by determining the membership values that are going to be processed in the decision system and then converting these crisp set data into a fuzzy set data. Next, the membership rules must be defined fittingly to represent the characteristics of the membership value. Once these values are processed, the get defuzzified and a decision is made accordingly. The whole of this procedure is known as a Fuzzy Inference System (FIS), and is represented in Figure 4.1.

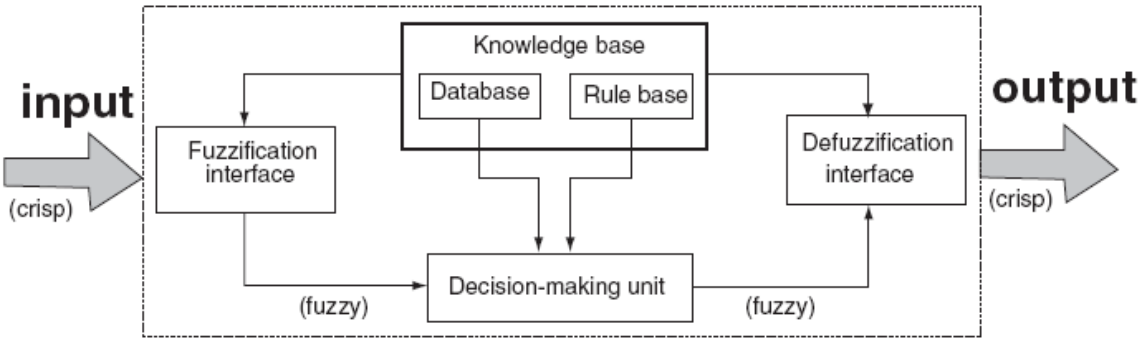

Figure 4.1 Fuzzy Inference System

4.1.2 Initialization of the Fuzzy Decision System

The fuzzy system is made up from a list of fuzzy sets as well as the rule set that they are associated with. The system is made up of two inputs and one output. Each input that the system takes is considered a fuzzy variable. Each of these inputs has their own membership functions, primarily constructed from trapezoidal and triangular functions.

The inputs to the system are used from the data acquired as a result of the step responses that were performed earlier on the EFC valves. One of the inputs is the current amplitude; 1.4A being defined as Low, and the other is 1.6 A being defined as High. The other input was constructed as a result of the equating a modified version of the root square mean error between the real response of the EFC valve and the simulated response of the EFC valve that was found in Chapter 2. Figures 4.2 through 4.6 are used to clarify the method in question. We can see that there are two responses, one generated as a result of simulated data (X_S), and the other generated as a result of the real data (X_R). Using these two variables we can come up with a value, representative of the modified version of the root mean square error (Equation 4.1) of a certain period of time. This value differs from EFC valve to EFC valve.

$$\overline{Error} = \frac{\sqrt{\sum_{i=1}^{N} \left(X_{R,i} - X_{S,i} \right)^2}}{t} \tag{4.1}$$

Where t is the time period, and N represents the amount of data points. The output is a conclusion of the fuzzy system where a decision is made for classifying the EFC valves' type.

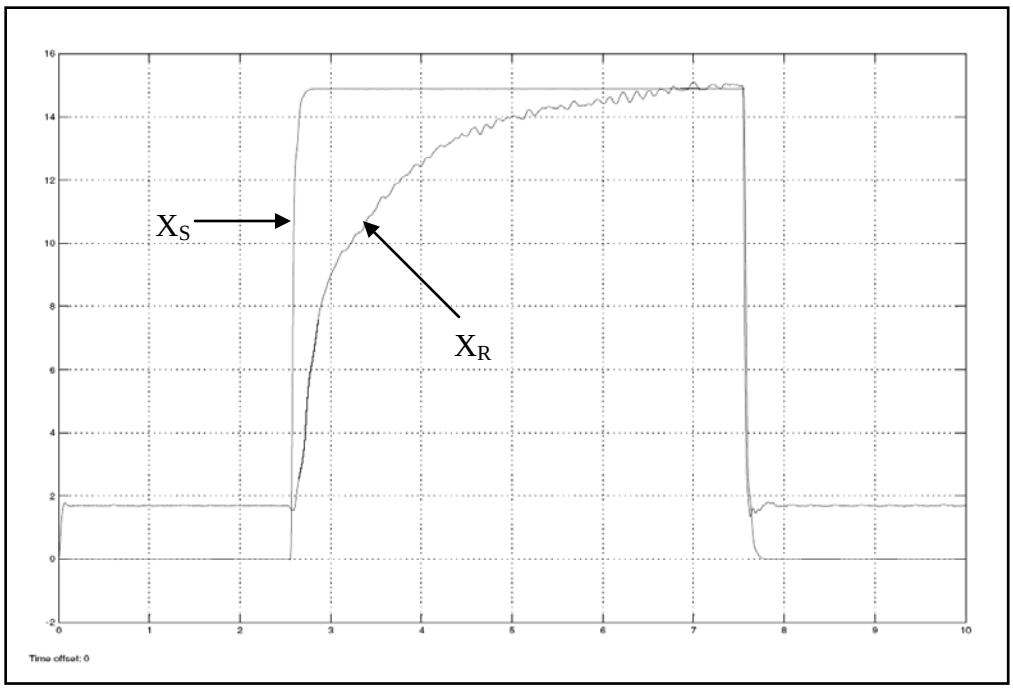

Figure 4.2 Return EFC Valve with 1.4 Amps current input

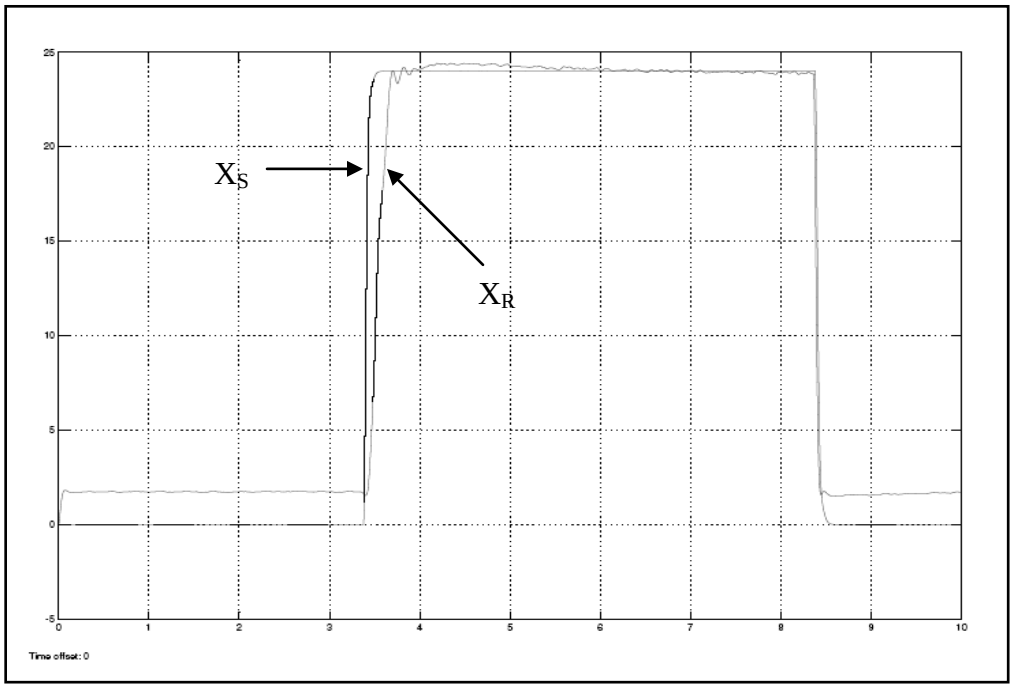

Figure 4.3 Good EFC Valve with 1.4 Amps current input

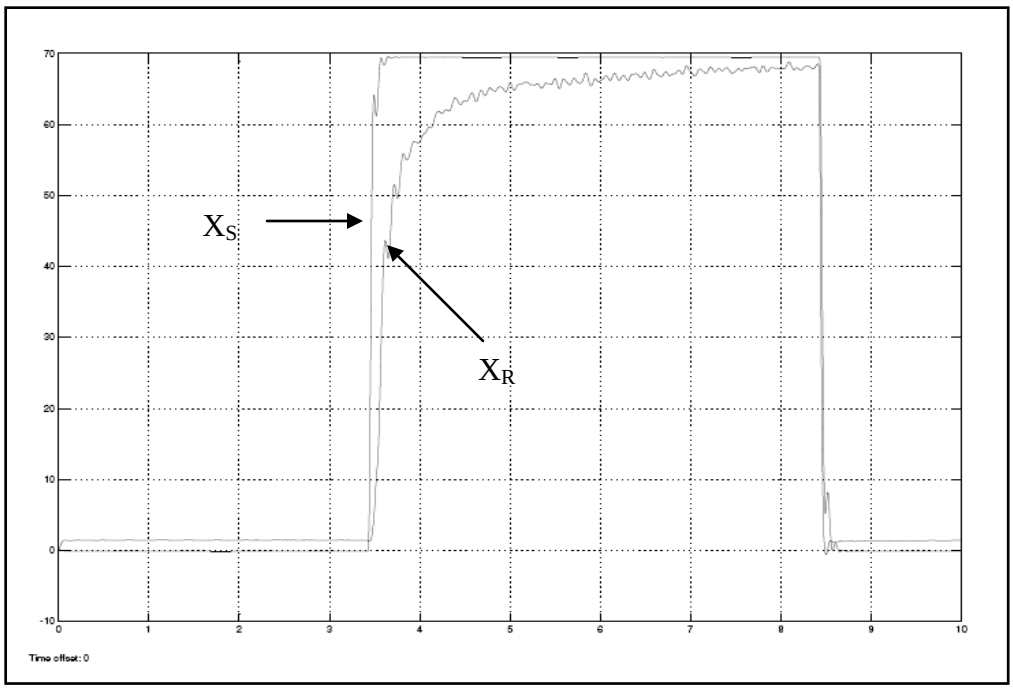

Figure 4.4 Return EFC Valve with 1.6 Amps current input

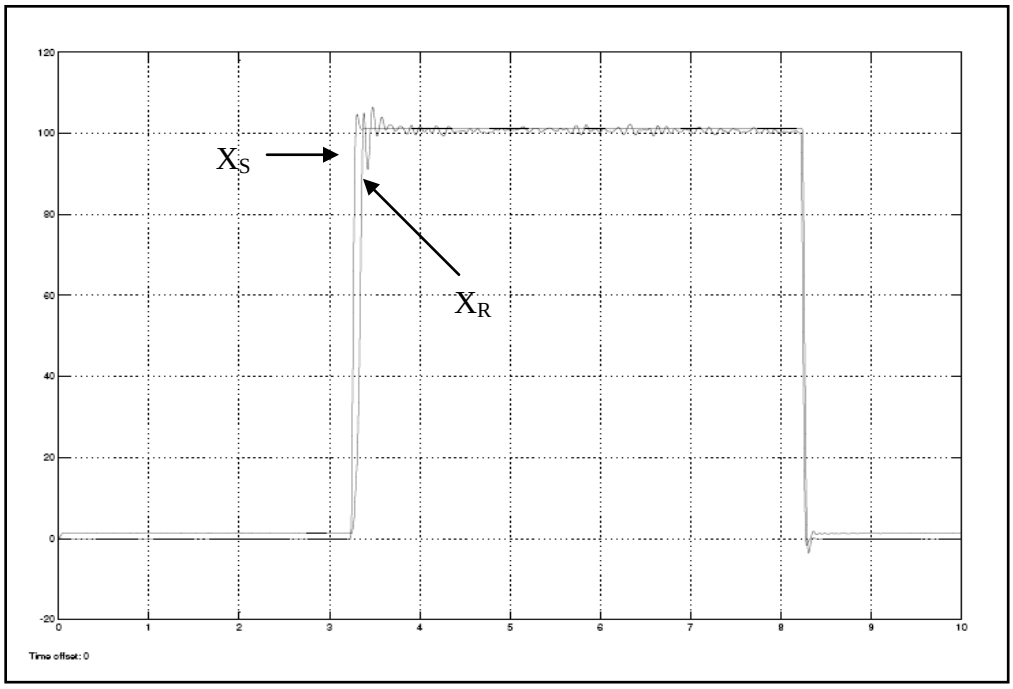

Figure 4.5 Good EFC Valve with 1.6 Amps current input

The membership functions of the fuzzy system used in this pattern classification procedure are left-trapezoid function, right-trapezoid function, and triangular function. Definitions of the membership functions are as follows,

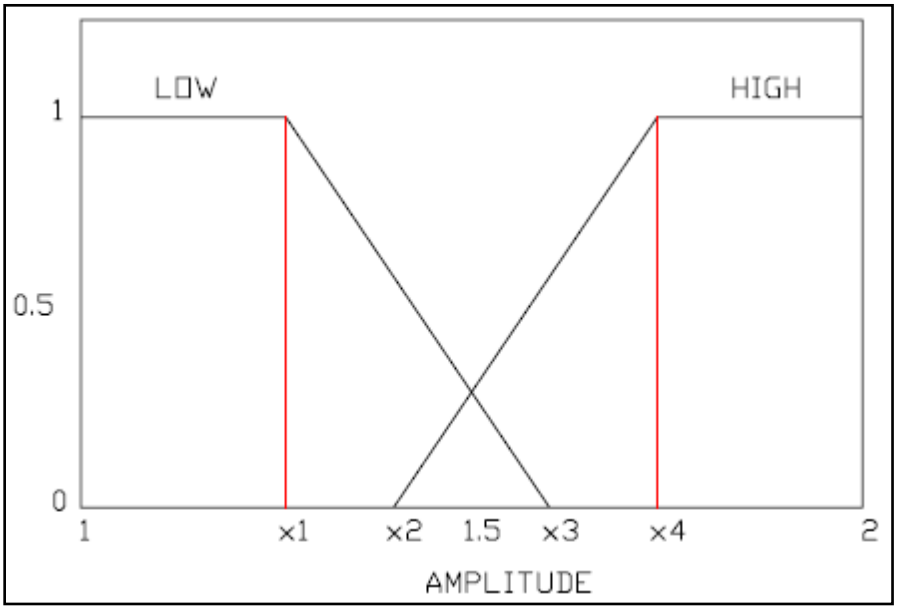

Figure 4.6 Two membership functions used in fuzzy system

$$f_{Left-Trapezoid}(x) = \begin{cases} 1 & x < x_1 \\ \dfrac{x_3 - x}{x_3 - x_1} & x_1 \le x < x_3 \\ 0 & x \ge x_3 \end{cases} \tag{4.2}$$

$$f_{Right-Trapezoid}(x) = \begin{cases} 0 & x < x_2 \\ \dfrac{x - x_2}{x_4 - x_2} & x_2 \le x < x_4 \\ 1 & x \ge x_4 \end{cases} \tag{4.3}$$

Where x_1 = 1.4 A, x_2 = 1.45 A, x_3 = 1.55 A, and x_4 = 1.6 A.

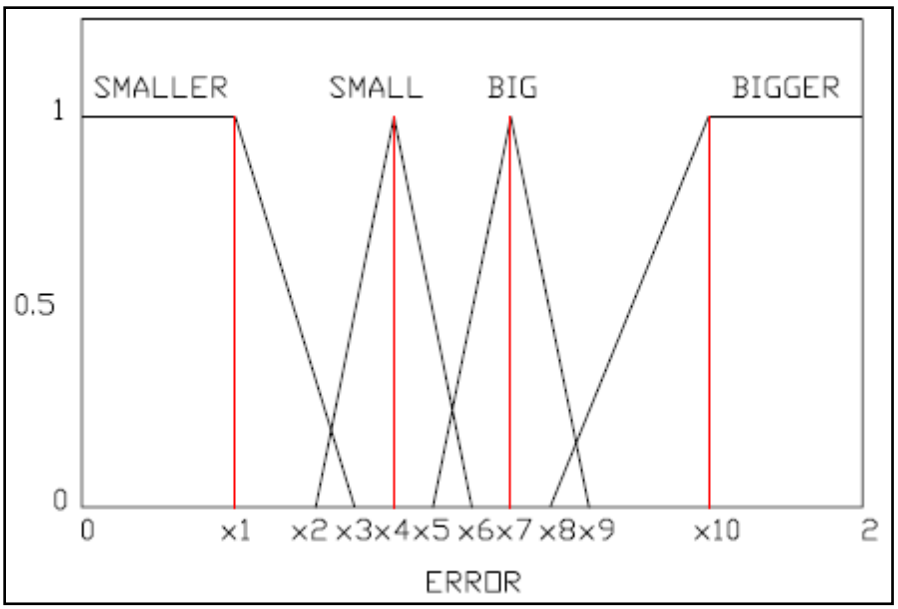

Figure 4.7 Four membership functions used in fuzzy system

$$f_{Left-Trapezoid}(x)=\begin{cases}1 & x<x_1\\ \dfrac{x_3-x}{x_3-x_1} & x_1\le x<x_3\\ 0 & x\ge x_3\end{cases} \tag{4.4}$$

$$f_{Left-Triangle}(x)=\begin{cases}\dfrac{x-x_2}{x_4-x_2} & x_2\le x<x_4\\ \dfrac{x_6-x}{x_6-x_4} & x_4\le x<x_6\end{cases} \tag{4.5}$$

$$f_{Right-Triangle}(x)=\begin{cases}\dfrac{x-x_5}{x_7-x_5} & x_5\le x<x_7\\ \dfrac{x_9-x}{x_9-x_7} & x_7\le x<x_9\end{cases} \tag{4.6}$$

$$f_{Right-Trapezoid}(x)=\begin{cases}0 & x<x_8\\ \dfrac{x-x_8}{x_{10}-x_8} & x_8\le x<x_{10}\\ 1 & x\ge x_{10}\end{cases} \tag{4.7}$$

Where $x_1 = 0.4$, $x_2 = 0.5$, $x_3 = 0.8$, $x_4 = 0.9$, $x_5 = 1.1$, $x_6 = 1.2$, $x_7 = 1.3$, $x_8 = 1.5$, $x_9 = 1.6$, and $x_{10} = 1.8$.

The fuzzy rules are based on a set of fuzzy if – then rules in order to define the inference system from the input data to the output data based on the knowledge of the characteristics of the EFC valve.

Once all the initializations have been met, the intended tests could be run. We are able to build the fuzzy system using MATLAB / Fuzzy Logic Toolbox and then use it in parallel with m-file scripts and Simulink models. The results are provided next.

4.1.3 Experimental Results

For verification purposes, this pattern classification technique was implemented on EFC valves that were classified previously. Four different types of EFC valves were used; two of them determine to be return (bad) valves, and two of them determined to be good valves. Data from the step responses are taken into consideration here, both for low current amplitude (1.4 A) and high current amplitude (1.6 A). From that data, the membership value (mean square root error) that will be used in the fuzzy system is calculated by using (4.1). Table 4.1 provides the EFC valves with their corresponding membership (error) values. From the pattern that these errors created the classification of the EFC valves were extended into three types: good, malfunctioned, and severely malfunctioned. In real life applications, the EFC valves that are returned to Cummins by their customers are primarily caused by functionality issues. Although an EFC valve characterized as malfunctioned as opposed to an EFC valve characterized as severely malfunctioned both fall under the class ‘return’, we are able to further distinguish them between each other by using fuzzy logic.

Table 4.1 Results of $\overline{Error}$ calculation

Serial #	Condition	Error	
		Low A	High A
16011093	New	1.0156	0.9048
		1.0030	0.9174
		1.0378	0.9229
		1.0396	0.8740
		1.0233	0.8837
		1.0611	0.8788
		1.0634	0.8328
		1.0476	0.9143
		1.0536	0.8498
		1.0249	0.9128
16011094	New	1.0025	0.8931
		0.9742	0.8553
		0.9740	0.8388
		0.9810	0.8046
		0.9746	0.8814
		0.9682	0.8076
		0.9704	0.8168
		0.9704	0.8321
		0.9793	0.7948
		0.9695	0.8158
15969045	Return	1.8048	1.0689
		1.8048	1.0659
		1.6242	1.0763
		1.5982	1.0706
		1.6573	1.1234
		1.6254	1.0779
		1.5485	1.1019
		1.6291	1.0546
		1.7645	1.0782
		1.6671	1.0934
15969046	Return	1.2697	0.9865
		1.2176	1.0326
		1.3267	1.0139
		1.3357	1.0078
		1.2477	0.9998
		1.2507	1.0061
		1.1917	1.0025
		1.2510	0.9852
		1.2268	1.0106
		1.2363	0.9862

The implementation of the fuzzy system was written in MATLAB. After the EFC test data was preprocessed we were in possession of 80 sets of data. Once the data was processed in the fuzzy system, the EFC valves were classified correctly, even furthering the categories to extreme conditions amongst each other. Basically, what was already determined to be a bad (return) valve was classified based on its pattern as either a malfunctioned EFC valve or a severely malfunctioned EFC valve. Figures 4.8 and 4.9 are the Simulink models used to process the data.

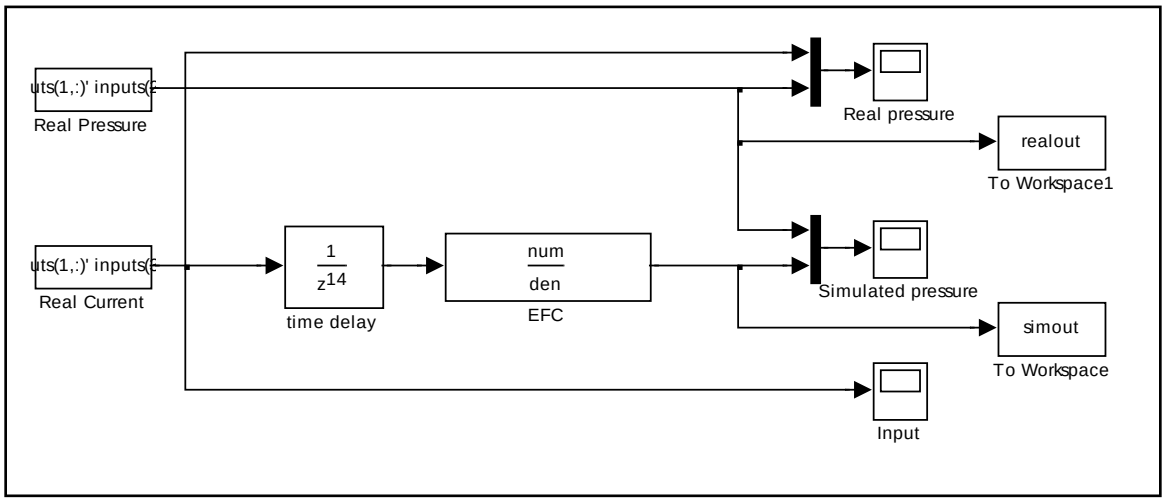

Figure 4.8 Model that processes the real data and simulated data

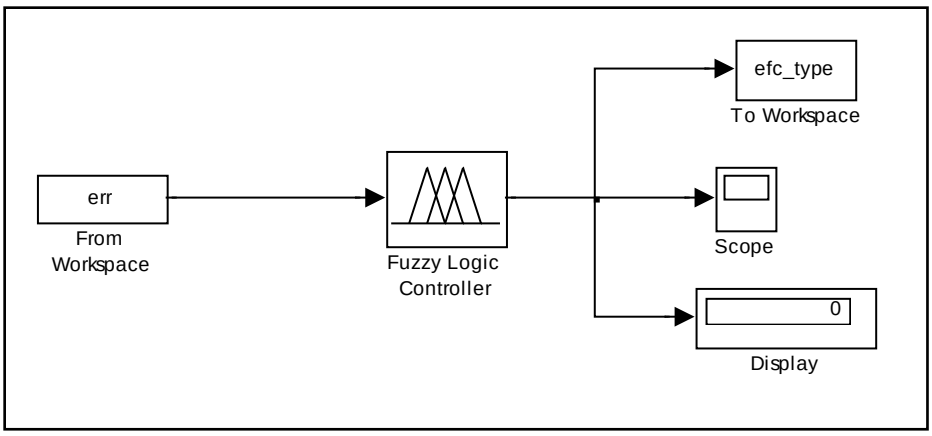

Figure 4.9 Model that implements the preprocessed data in the fuzzy system

On a few instances concerning the data acquired from the good EFC valve, there were overlaps on the parameters making up the membership functions. Although fundamentally they are still classified accurately as good EFC valves, there were unavoidable consequences from the data due to noise and unforeseen responses. The degrees of memberships took over a categorized these EFC valves in their respective classes. Table 4.2 provides the results after the training data was processed in the fuzzy system. These classes are a result of the defuzzification procedure. For the defuzzification process, based on the ranges that the error values fell under, the EFC Valves were classified according to the following rules:

$$f_{class\_low}(error) = \begin{cases} Good & \overline{error} < 1.065 \\ Malfunctioned & 1.065 \le \overline{error} < 1.535 \\ Severely\ Malfunctioned & 1.535 \le \overline{error} \end{cases}$$

$$f_{class\_high}(error) = \begin{cases} Good & \overline{error} < 0.923 \\ Malfunctioned & 0.923 \le \overline{error} < 1.041 \\ Severely\ Malfunctioned & 1.041 \le \overline{error} \end{cases}$$

Table 4.2 Classification of EFC Valves after fuzzy logic reasoning

Serial #	Condition	Error	
		Low A	High A
16011093	New	Good	Good
		Good	Good
		Good	Good
		Good	Good
		Good	Good
		Good	Good
		Good	Good
		Good	Good
		Good	Good
		Good	Good
16011094	New	Good	Good
		Good	Good
		Good	Good
		Good	Good
		Good	Good
		Good	Good
		Good	Good
		Good	Good
		Good	Good
		Good	Good
15969045	Return	Severely Malf.	Severely Malf.
		Severely Malf.	Severely Malf.
		Severely Malf.	Severely Malf.
		Severely Malf.	Severely Malf.
		Severely Malf.	Severely Malf.
		Severely Malf.	Severely Malf.
		Severely Malf.	Severely Malf.
		Severely Malf.	Severely Malf.
		Severely Malf.	Severely Malf.
		Severely Malf.	Severely Malf.
15969046	Return	Malfunctioned	Malfunctioned
		Malfunctioned	Malfunctioned
		Malfunctioned	Malfunctioned
		Malfunctioned	Malfunctioned
		Malfunctioned	Malfunctioned
		Malfunctioned	Malfunctioned
		Malfunctioned	Malfunctioned
		Malfunctioned	Malfunctioned
		Malfunctioned	Malfunctioned
		Malfunctioned	Malfunctioned

When we take a look at the classification results, it is evident that a pattern exists between good EFC valves and bad (return) EFC valves. Furthermore, this pattern allows us to distinguish amongst the EFC valves depending on their functionality conditions. The fuzzy system is able to satisfy the pattern classification for both low amplitude input, as well as high amplitude inputs. The fuzzy system classified the types of the EFC valves correctly for 80 different sets of data, and it only made 4 “soft” errors for the classifications between the functionality conditions.

5 CONCLUSIONS AND RECOMMENDATIONS

5.1 Conclusions

The system modeling of the EFC valves was developed in order to determine a relationship between the input, Voltage, V, and the output, Pressure, P, of the system. The dynamics of the electrical part and the mechanical part of the EFC valve were taken into account and combined to come up with the model. It was further proved that the linearization of the model was possible to obtain.

There were drawbacks to this approach, however, mainly because of the complexity of the system as well as the data lost throughout the design and development of the EFC Actuator. At the post – production portion of the EFC Actuator, manual fixes are a common trend, mainly in the adjustment of the spring loads that keep the EFC valve is a normally open or normally closed state. Another variable that should be considered in the model is the discharge coefficient of the valve shaft, which was information that was unable to be provided by the supplier of the EFC Actuator.

The system identification of the EFC valves proved to be more effective. Two types were considered: Frequency Domain and Time Domain. In the frequency domain approach, the transfer function was roughly estimated to be around 8^{th} and 9^{th} order. The transfer functions of the models were estimated, only to find that the coefficients were small and sensitive enough to make a significant impact on the results of Bode Plots (Sections 3.1.3.1 and 3.2.1.3). Furthermore, this was a trial and error approach that proved to be tedious and cumbersome at best.

The aforementioned transfer functions were also estimated using the Recursive Least Squares (RLS) method (Section 3.2.2.2). Using this methodology, we were able to come up with an estimation of the EFC valves in discrete time domain. This did not appear to be an effective approach because the coefficients making up the transfer functions of the EFC valves did not maintain a certain pattern within each category of the EFC valve. The contribution of leakage in the design of the EFC valve was causing a discrepancy between the different types of EFC valves. Also, the "stickiness" phenomenon was causing the valve opening and closing to behave in an unstable manner between the different types of EFC valves that were experimented with.

The approach in time domain proved to be far more efficient and effective with the use of step response. The characteristics of the curves from the responses became evident when using different types of EFC valves that were predetermined to be good valves or bad valves (Section 3.1.3.2). The decision to use inputs of different amplitude levels proved to be fruitful, especially for low current (1.4 A), and high current (1.6 A). The responses showed that good EFC valves had fast rise time, compared to bad EFC valves that had slow rising time. Also, the settling portion demonstrated oscillations for the bad EFC valves, compared to the good EFC valves, which did not.

Fuzzy Logic was implemented for the purposes of pattern classification. Each type of EFC valve demonstrated to carry a certain pattern in the form of a modified version of the root mean square error (Equation 4.1). This, along with current input was used in the fuzzy system in order to classify the type of EFC valve being tested. This method proved to be very effective, as all the types of EFC valves that were already pre-classified, were verified accurately for their respective types.

5.2 Recommendations for Future Work

There is some more work that can be done in the future to improve the dynamic testing method of the EFC valves as shown below.

- More material tests [19; 20] need to be conducted in order to find the values for the discharge coefficient valve shaft, the inertia value caused by the rotation of the shaft, the spring loads, damping coefficient, friction torque, and the leakage rate. The information of these values will help determine an accurate model of the EFC valve.

- Further system identification methods have to be explored, perhaps combining multiple methods for verification purposes, or using one method from frequency domain and another from time domain in order to reinforce one another [21].

LIST OF REFERENCES

LIST OF REFERENCES

[1] Electric Fuel Control Governor Familiarization, Cummins Engine Company, Inc., Columbus, IN, 1986.

[2] L. Schruben and V. Cogliano, "An Experimental Procedure for Simulation Response Surface Model Identification," *Communications of the Association for Computing Machinery,* Vol. 30, No. 8, pp. 716-730, 1987.

[3] S. Jacobson, "Discrete-Event Computer Simulation Response Optimization in the Frequency Domain," PhD Thesis, School of Operations Research and Industrial Engineering, Cornell University, Ithaca, NY.

[4] R. Pintelon and J. Schoukens, "Frequency Domain System Identification with Missing Data," *IEEE Transactions on Automatic Control,* Vol. 45, No. 2, pp. 364-369, 2000.

[5] B. Gustavsen and A. Semlyen, "A Robust Approach for System Identification in the Frequency Domain," *IEEE Transactions on Power Delivery,* Vol. 19, No. 3, pp. 1167-1173, 2004.

[6] S. E. Lyshevski, "Identification of Nonlinear Systems with Noisy Data: A Nonlinear Mapping – Based Concept in Time Domain," *Proceedings of the American Control Conference,* Vol. 2, pp. 1634-1635, 2001.

[7] I. Gustavsson, L. Ljung, and T. Soderstrom, "Identification of Processes in Closed Loop-Identifiability and Accuracy Aspects," *Automatica,* Vol. 13, No. 59, 1977.

[8] K. J. Astrom and B. Wittenmark, "Self Tuning Controllers Based on Pole-Zero Placement," *IEEE Proceedings D,* Vol. 127, Issue 3, pp. 120-130, 1980.

[9] P. Young, *Recursive Estimation and Time Series Analysis – An Introduction,* Berlin: Springer-Verlag, 1984.

[10] K. C. A. Smith and R. E. Alley, "Electrical Circuits – An Introduction," *Cambridge University Press,* 1992.

[11] R. C. Dorf and R. H. Bishop, *Modern Control Systems 10th Edition.* New Jersey: Pearson Prentice Hall, 2004.

[12] K. Ogata, *Modern Control Engineering, 5th Edition.* New Jersey: Prentice Hall, 2010.

[13] Operator's Manual – EFC Test Stand, 38078, Cummins Engine Company, Inc., Columbus, IN, 1995.

[14] Performance Specification – Actuator, ETR Fuel Control, 14111, Cummins Engine Company, Inc., Columbus, IN.

[15] R. Pintelon, P. Guillaume, Y. Rolain, J. Schoukens, and H. Van Hamme, "Parametric Identification of Transfer Functions in the Frequency Domain, a Survey," *IEEE Transaction in Automatic Control,* Vol. 39, No. 11, pp. 2245-2260, 1994.

[16] P. Santos and J. L. Martins, "Automatic Transfer Function Synthesis from a Bode Plot," *IEEE Proceedings on Decision and Control,* Vol. 2, pp. 1093-1098, 1990.

[17] S. N. Sivanandam, S. Sumathi, and S. N. Deepa, *Introduction to Fuzzy Logic using MATLAB,* Berlin: Springer-Verlag, 2007.

[18] Y. Zhu, X. Lin, Y. Chen, and R. Eberhart, "Fuzzy Diagnostic System for EV Traction Battery Pack," *18th International Battery, Hybrid and Fuel Cell Electric Vehicle Symposium and Exhibition,* Berlin, Germany, 2001.

[19] S. R. Lee and K. Srinivasan, "On-line Identification of Process Models on Closed Loop Material Testing," *Proceedings of the American Control Conference,* Vol. 88, pt. 1 - 3, pp. 1909 – 1916, 1988.

[20] G. Money, "Material Testing and Characterization: Analysis, Innovation, and Results," *Powder Handling and Processing,* Vol. 19, No. 1, pp. 52 – 54, 2007.

[21] M. Haroon and D. E. Adams, "Time and Frequency Domain Nonlinear System Characterization for Mechanical Fault Identification," *Nonlinear Dynamics,* Vol. 50, No. 3, pp. 387 – 408, 2007.

APPENDIX

APPENDIX STEP RESPONSES (1.2 Amps – 2.0 Amps)

The following figures represent the various types of characteristics demonstrated by the various types of EFC valves used. The figures have the step responses of the real pressure data, X_R, and the simulated pressure data, X_S. These are the responses of failed EFC valves and good EFC valves for various amplitudes of current inputs. Three sets of data have been collected for each EFC valve.

A.1 1.2 Amps Current Input

A.1.1 Failed EFC Valve

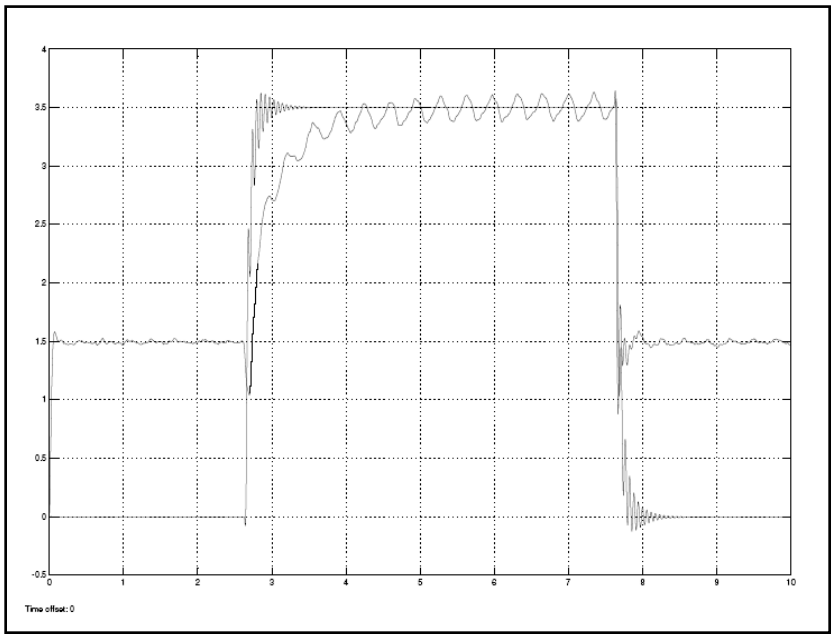

Figure A.1.1.a Pressure vs. Current plot for step response data set 1

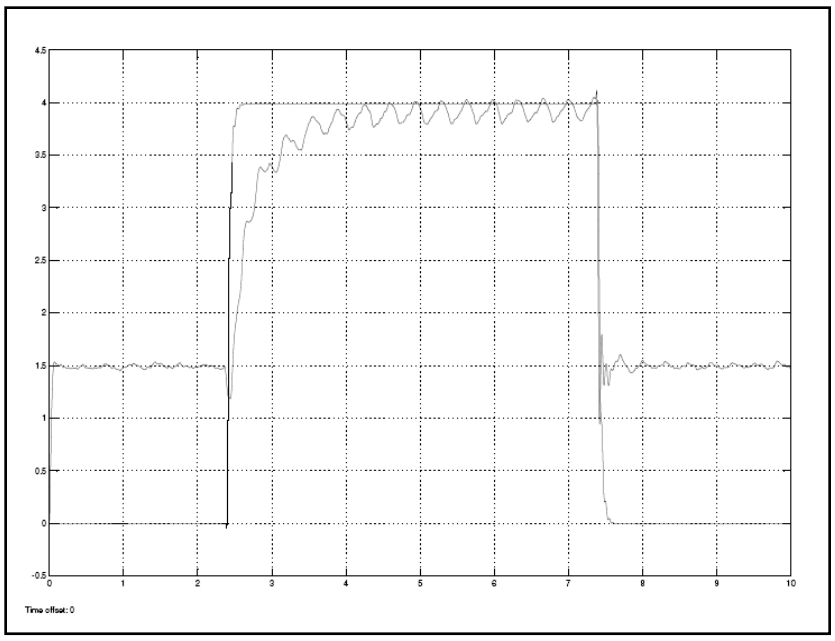

Figure A.1.1.b Pressure vs. Current plot for step response data set 2

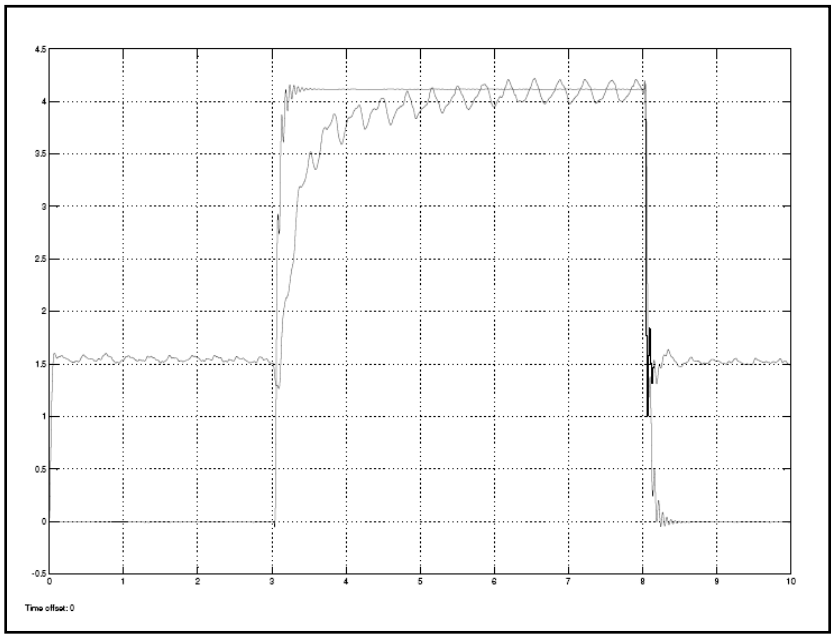

Figure A.1.1.c Pressure vs. Current plot for step response data set 3

A.1.2 Good EFC Valve

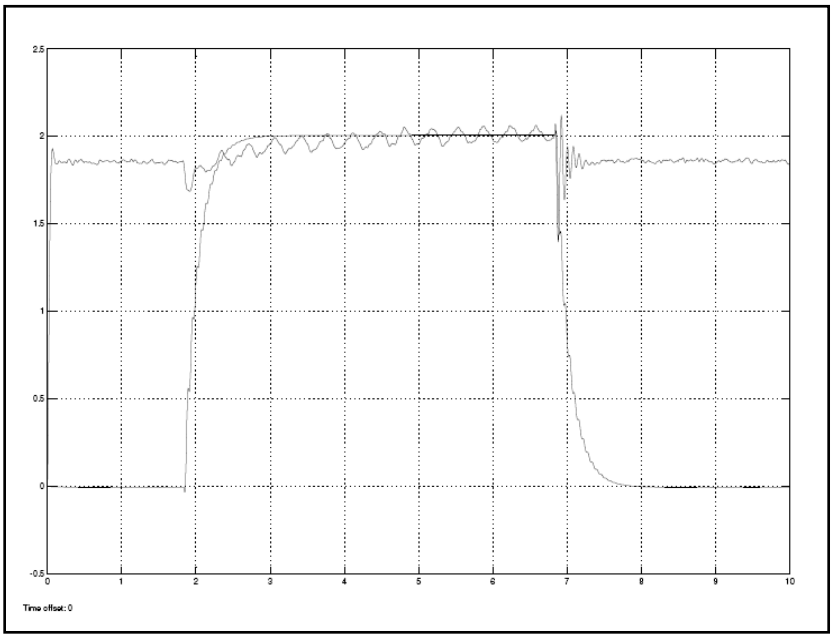

Figure A.1.2.a Pressure vs. Current plot for step response data set 1

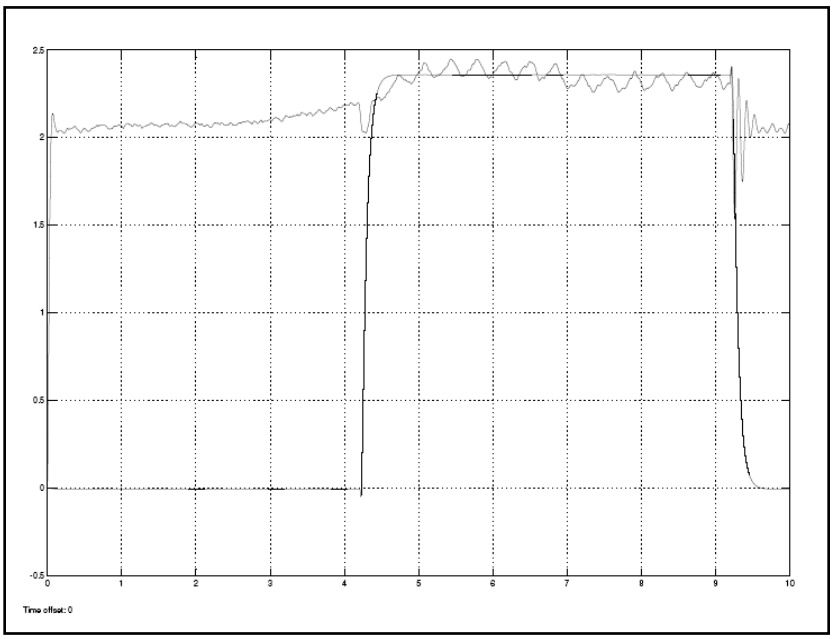

Figure A.1.2.b Pressure vs. Current plot for step response data set 2

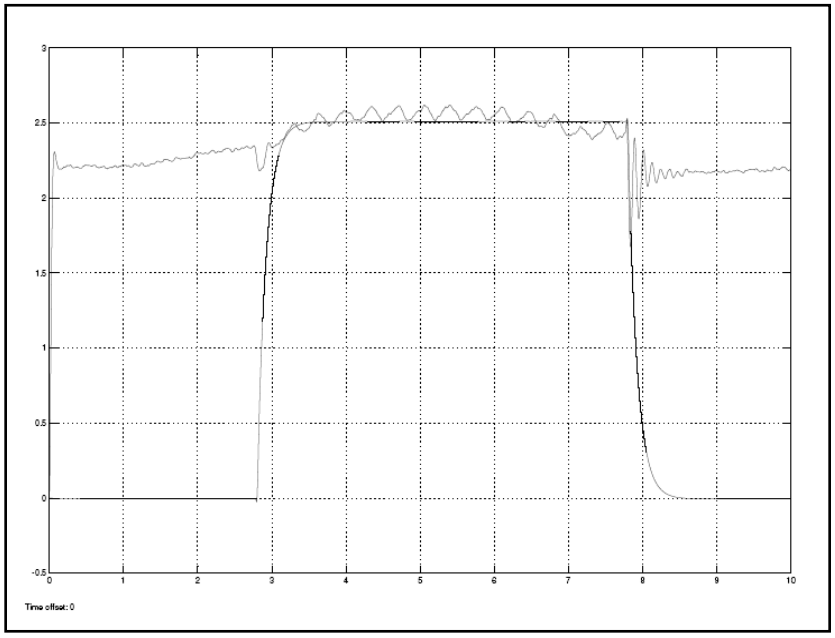

Figure A.1.2.c Pressure vs. Current plot for step response data set 3

A.2 1.4 Amps Current Input

A.2.1 Failed EFC Valve

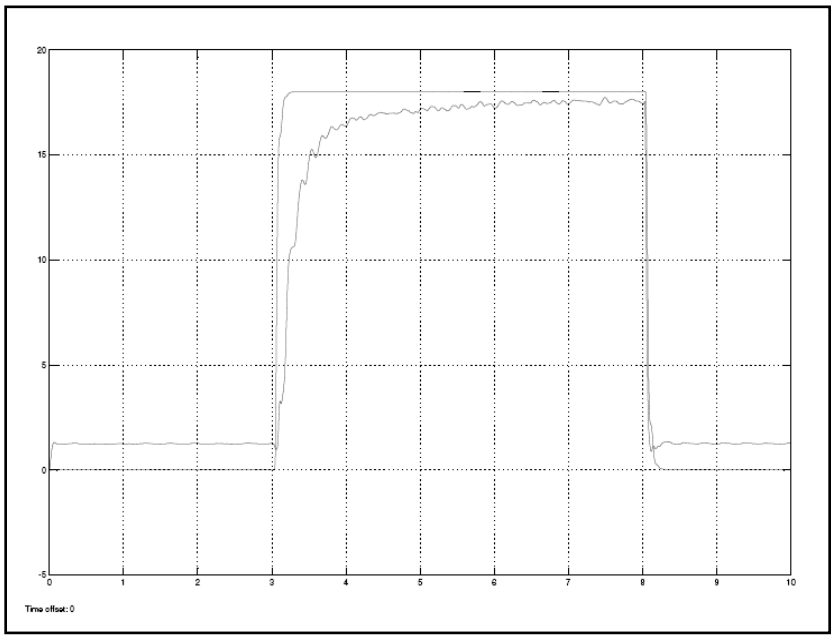

Figure A.2.1.a Pressure vs. Current plot for step response data set 1

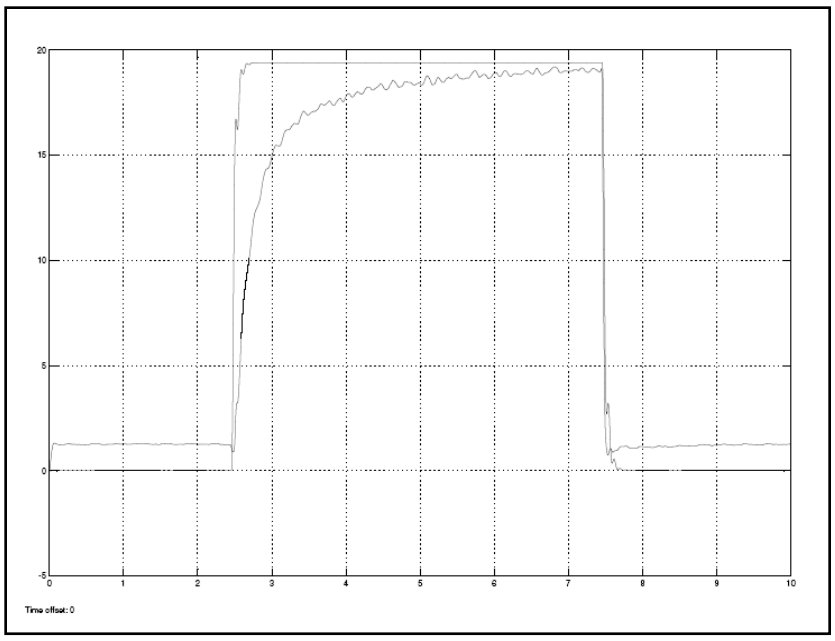

Figure A.2.1.b Pressure vs. Current plot for step response data set 2

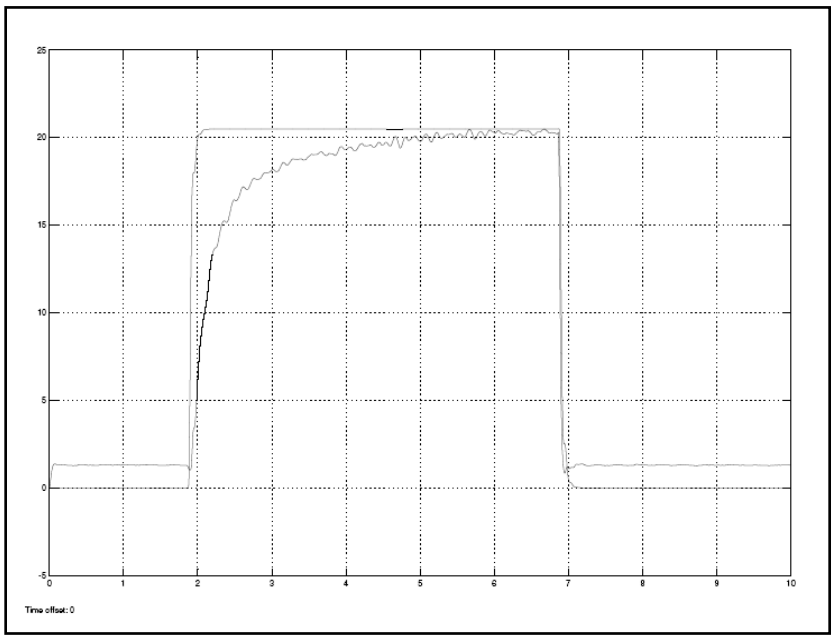

Figure A.2.1.c Pressure vs. Current plot for step response data set 3

A.2.2 Good EFC Valve

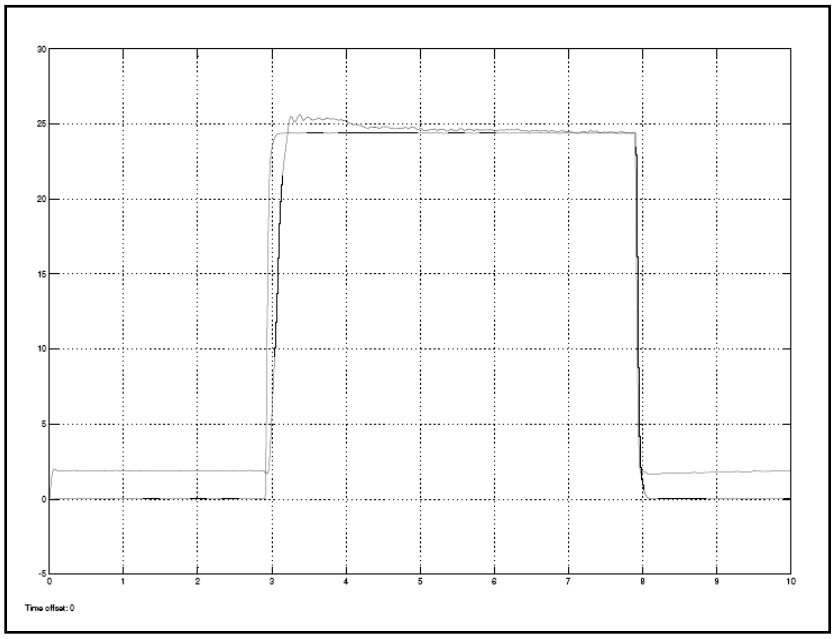

Figure A.2.2.a Pressure vs. Current plot for step response data set 1

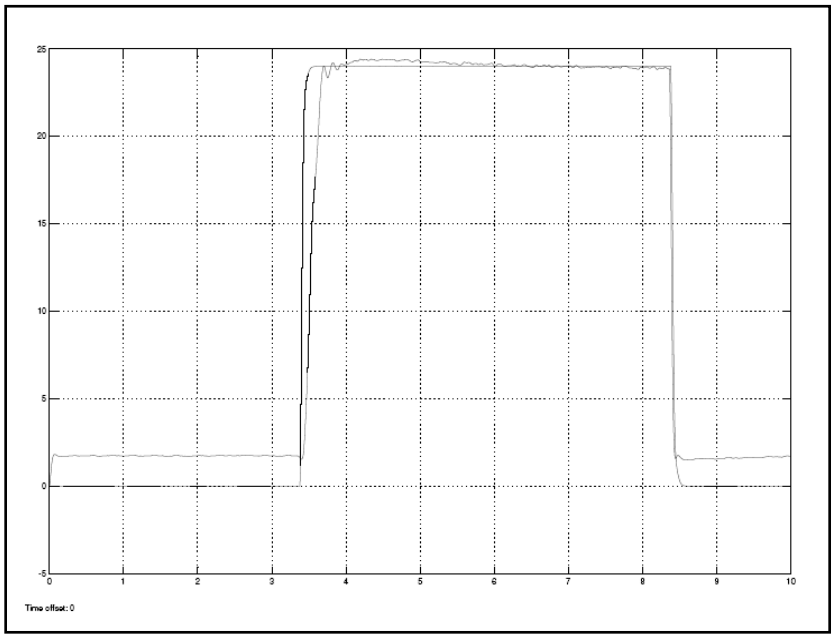

Figure A.2.2.b Pressure vs. Current plot for step response data set 2

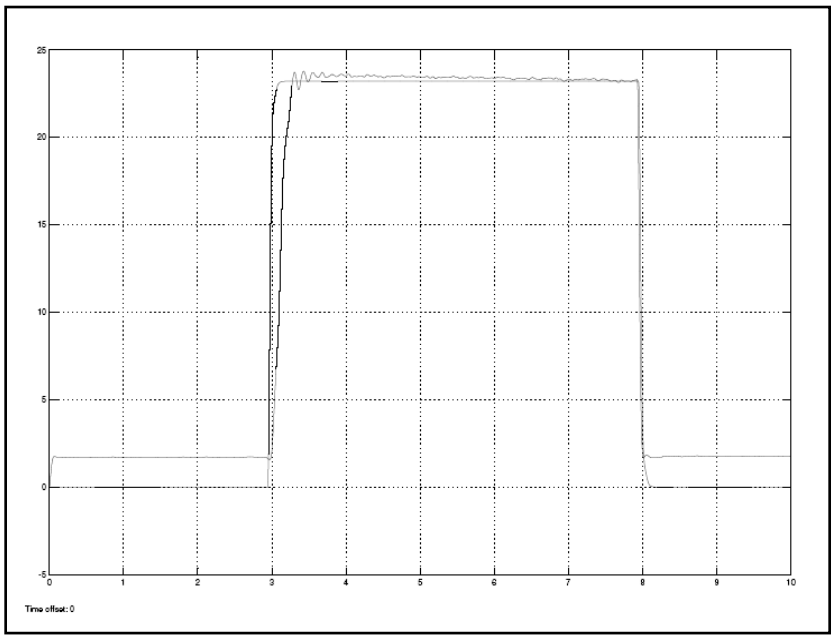

Figure A.2.2.c Pressure vs. Current plot for step response data set 3

A.3 1.6 Amps Current Input

A.3.1 Failed EFC Valve

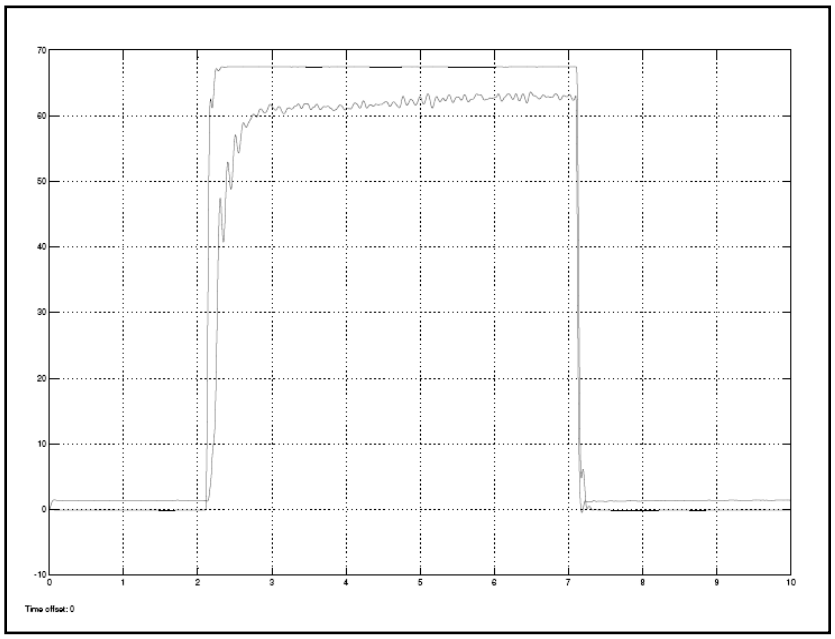

Figure A.3.1.a Pressure vs. Current plot for step response data set 1

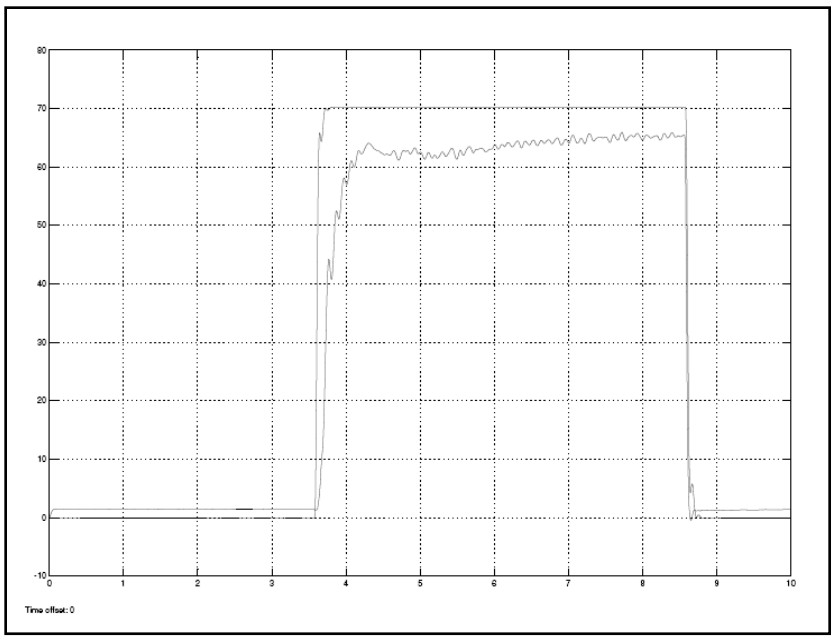

Figure A.3.1.b Pressure vs. Current plot for step response data set 2

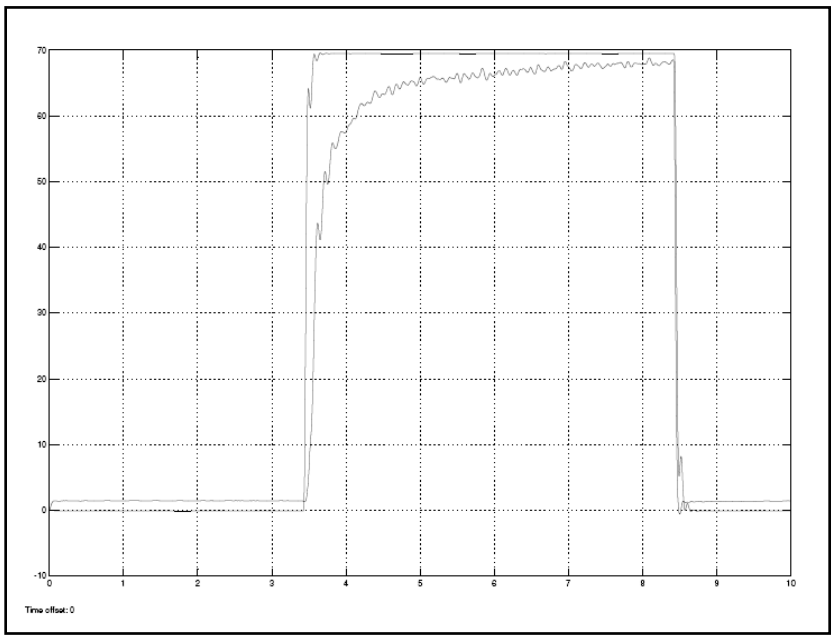

Figure A.3.1.c Pressure vs. Current plot for step response data set 3

A.3.2 Good EFC Valve

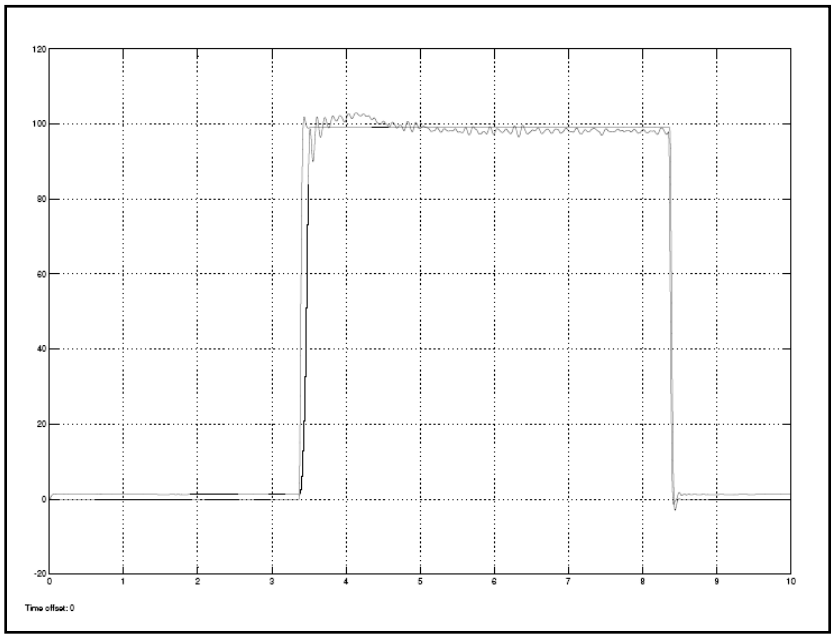

Figure A.3.2.a Pressure vs. Current plot for step response data set 1

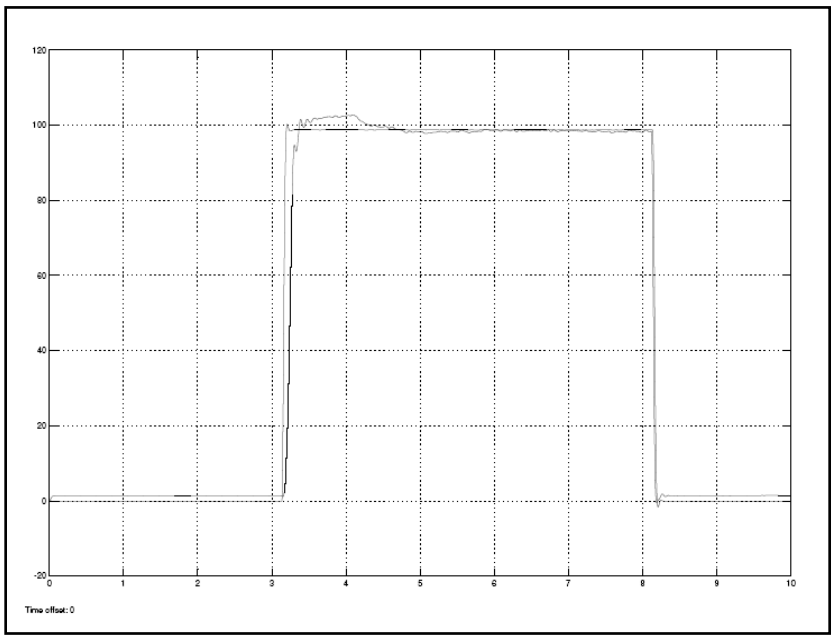

Figure A.3.2.b Pressure vs. Current plot for step response data set 2

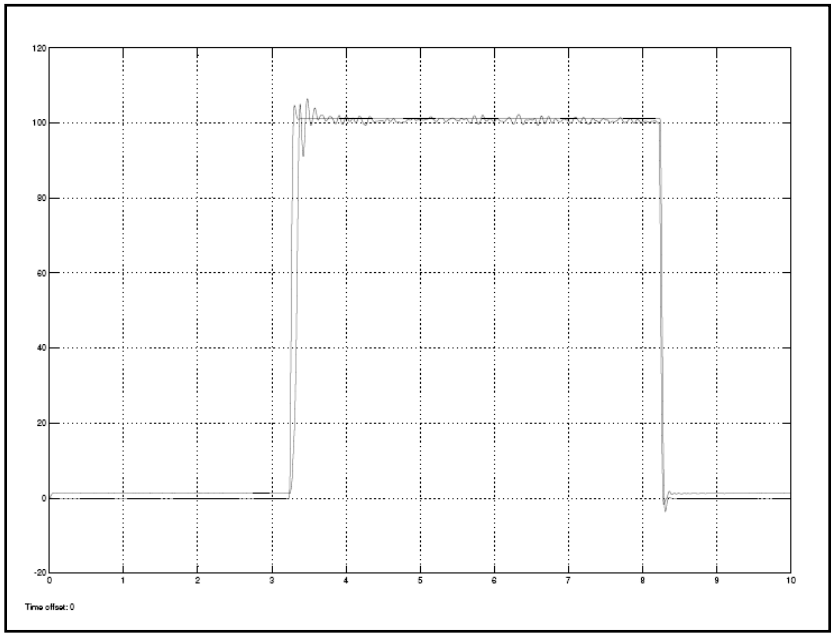

Figure A.3.2.c Pressure vs. Current plot for step response data set 3

A.4 1.8 Amps Current Input

A.4.1 Failed EFC Valve

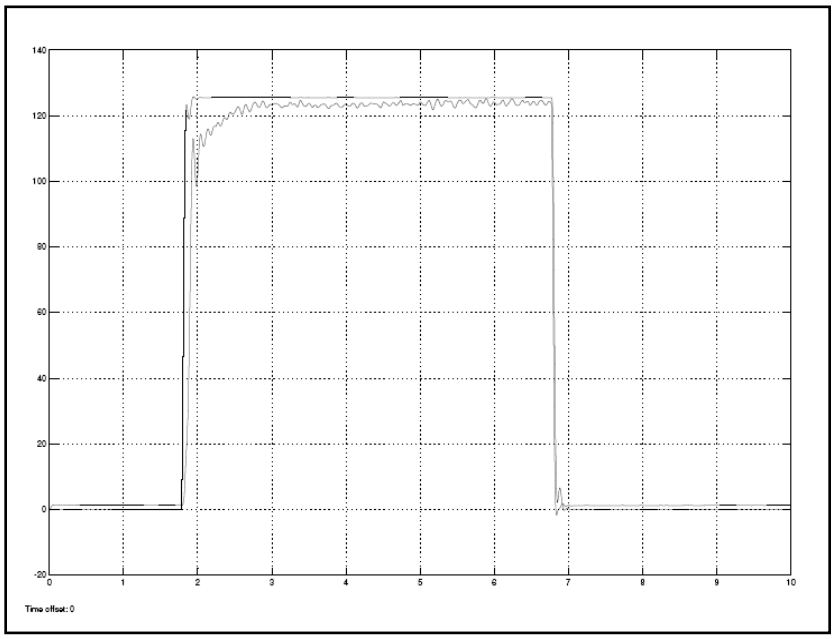

Figure A.4.1.a Pressure vs. Current plot for step response data set 1

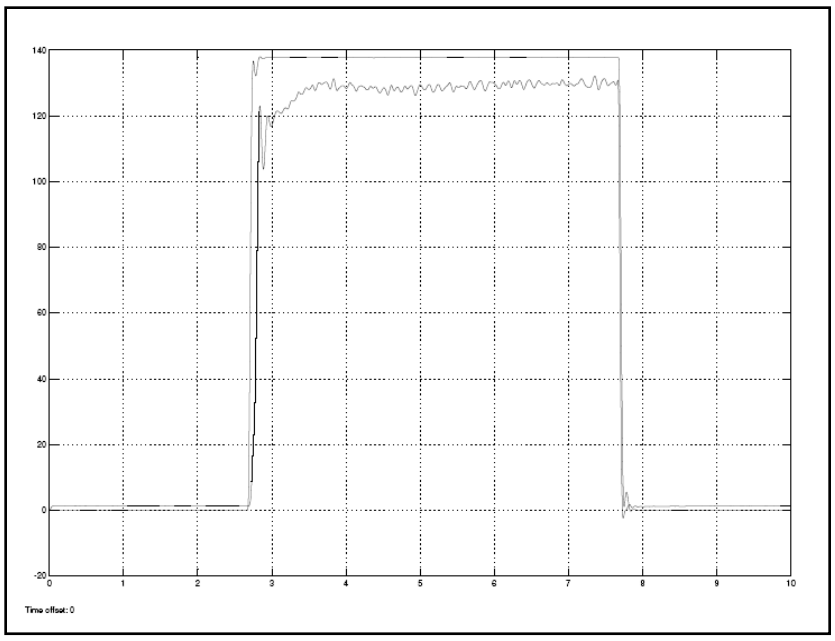

Figure A.4.1.b Pressure vs. Current plot for step response data set 2

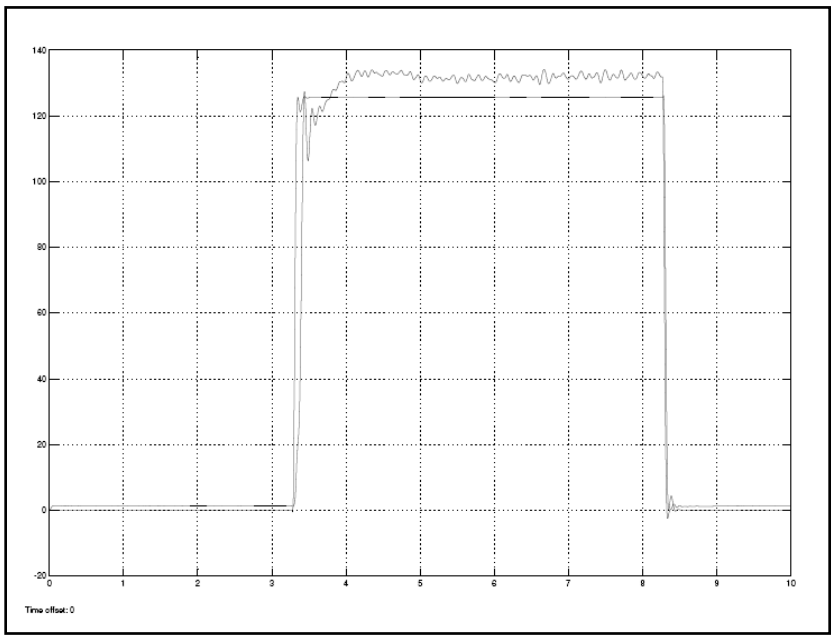

Figure A.4.1.c Pressure vs. Current plot for step response data set 3

A.4.2 Good EFC Valve

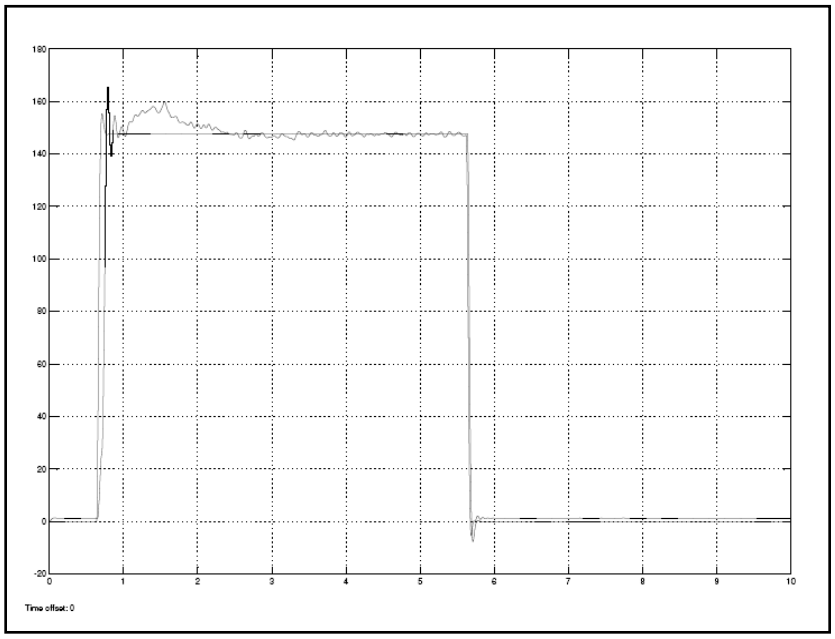

Figure A.4.2.a Pressure vs. Current plot for step response data set 1

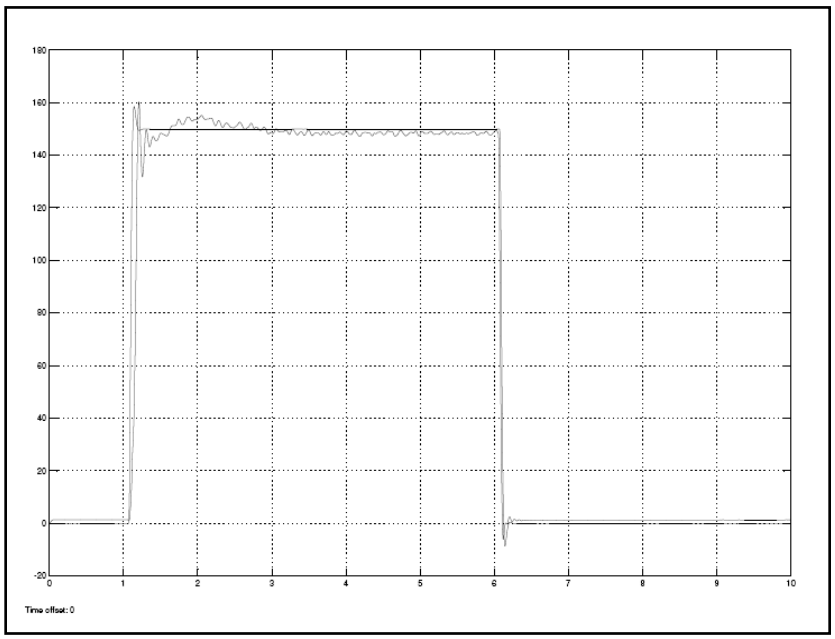

Figure A.4.2.b Pressure vs. Current plot for step response data set 2

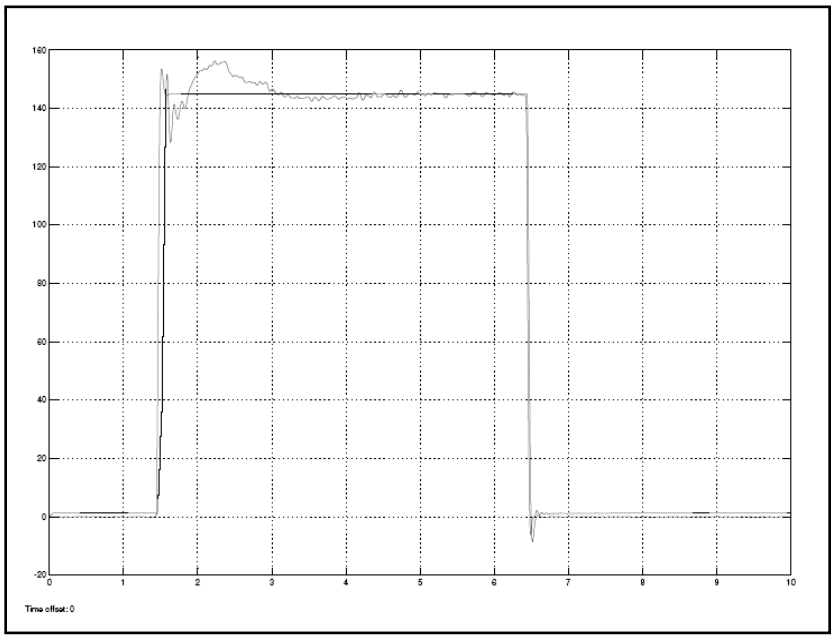

Figure A.4.2.c Pressure vs. Current plot for step response data set 3

A.5 2.0 Amps Current Input

A.5.1 Failed EFC Valve

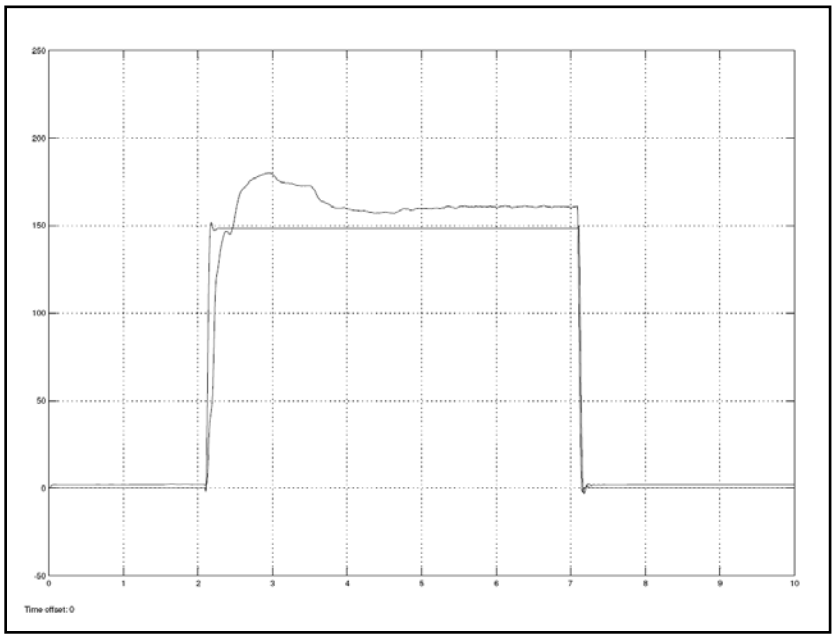

Figure A.5.1.a Pressure vs. Current plot for step response data set 1

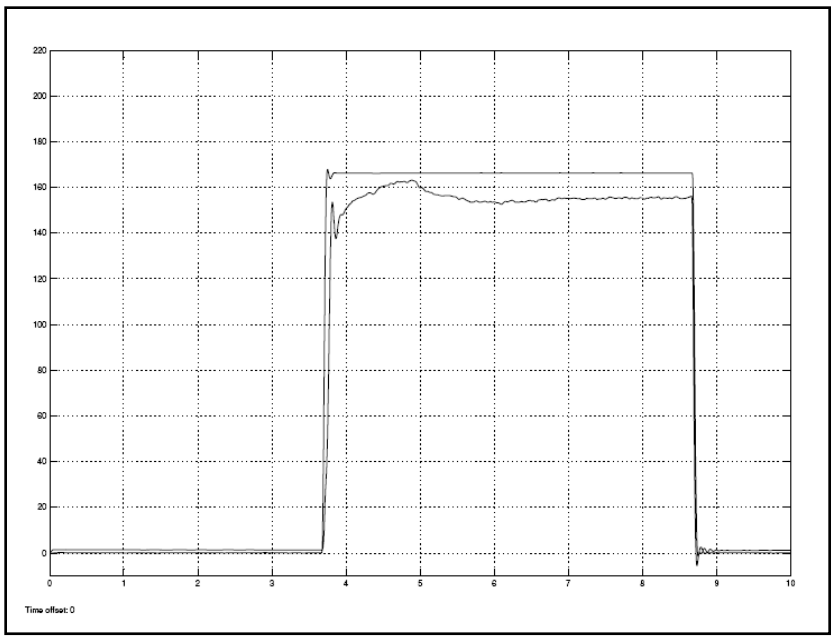

Figure A.5.1.b Pressure vs. Current plot for step response data set 2

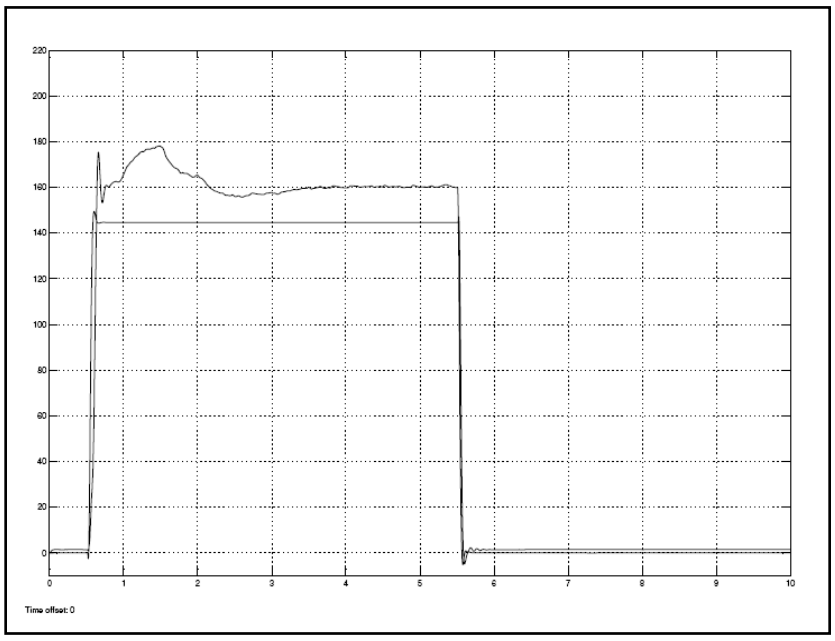

Figure A.5.1.c Pressure vs. Current plot for step response data set 3

A.5.2 Good EFC Valve

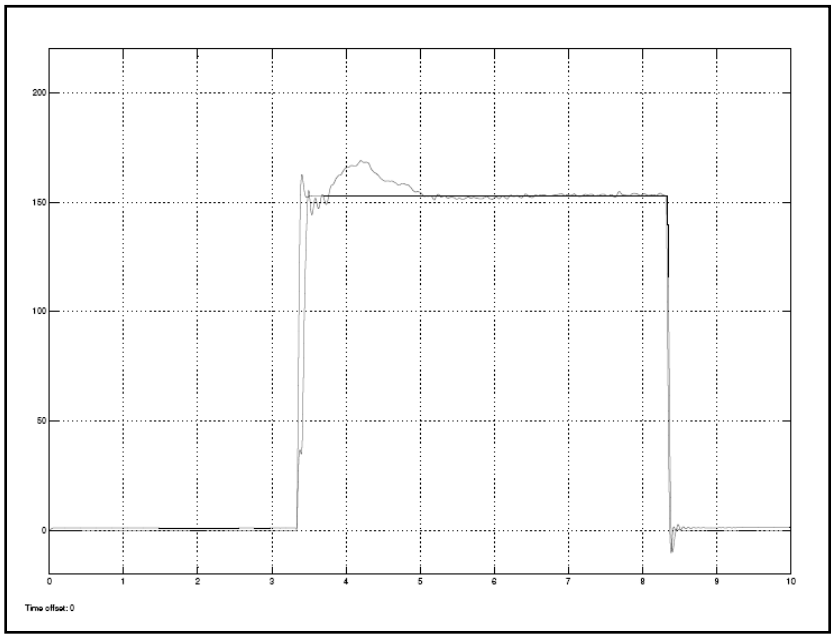

Figure A.5.2.a Pressure vs. Current plot for step response data set 1

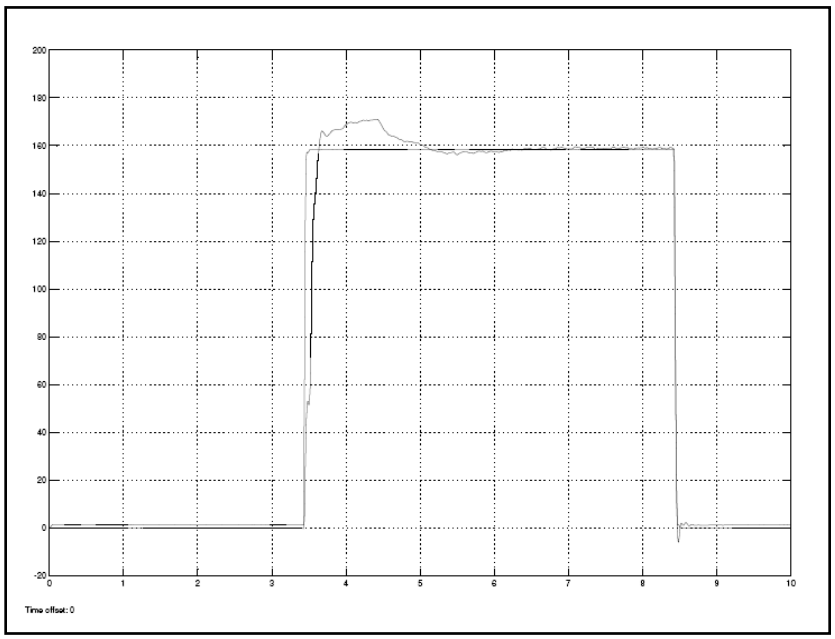

Figure A.5.2.b Pressure vs. Current plot for step response data set 2

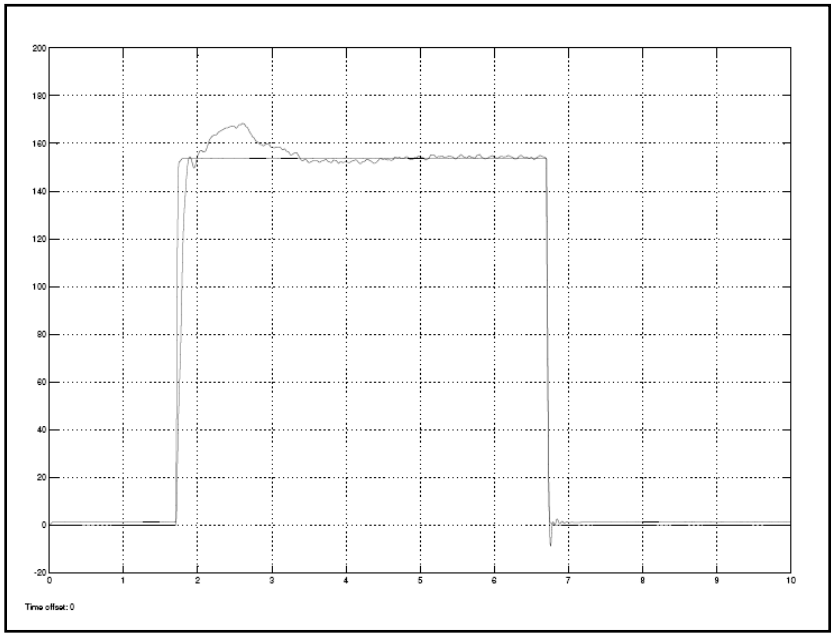

Figure A.5.2.c Pressure vs. Current plot for step response data set 3